Development and characterization of a novel inorganic polyphosphate-loaded hydrogel for immunomodulation of early fracture healing

Rayan Ben Letaifa

Division of Surgical and Interventional Sciences
Department of Surgery
Faculty of Medicine and Health Sciences
McGill University
Montreal, QC, Canada

A thesis submitted to McGill University in partial fulfillment of the requirements of the degree of Master of Science in Surgical and Interventional Sciences

First published on December 30th, 2024.

Table of Contents

Abstract ***4***

Résumé ***5***

Acknowledgements ***6***

List of Figures and Tables ***8***

Abbreviations ***8***

Contributions of Authors ***12***

Chapter 1: Introduction ***14***

Chapter 2: Literature Review ***17***

2.1 Inorganic Polyphosphates ***17***

2.1.1. Origin and Evolutionary Role ***17***

2.1.2. Chemical Structure ***18***

2.1.3. Multifunctional Role in Biology ***19***

2.1.4. Applications of polyP in bone and cartilage regeneration ***20***

2.1.5. Quantification of inorganic polyphosphates in the life sciences ***21***

2.2. Fracture Healing ***24***

2.2.1. Stages of fracture healing ***24***

2.2.2. The role of immune cells in fracture healing ***27***

2.2.3. Fracture complications ***30***

2.2.4. Fracture management and treatment ***31***

2.3. Hydrogels ***31***

2.3.1. Hydrogels for Drug Release 32

2.3.2. Mechanisms of network formation..... 32

2.3.3. Hydrogels for Fracture Healing Applications 34

2.3.4. Poloxamer and Gellan gum-based hydrogels 34

2.3.5. PolyP-releasing hydrogels 35

Chapter 3: Novel thermoresponsive and injectable inorganic polyphosphate-releasing hydrogel for fracture healing applications 37

3.1. Abstract..... 37

3.2. Introduction..... 38

3.3. Materials and Methods 41

3.4. Results..... 49

3.5. Discussion..... 63

3.6. Conclusion..... 69

Chapter 4: Discussion..... 71

Chapter 5: Conclusion and Summary..... 80

Bibliography..... 81

Abstract

Fractures are among the most prevalent musculoskeletal injuries. In the years 2015-2016 alone, there were a total of 130,000 fractures in Canada, which were associated with significant morbidity and healthcare expenses. Approximately 5-10% of fracture patients will incur fracture complications such as non- and mal- unions. These complications typically require invasive revision surgeries; however, they are not always successful. The incidence of fractures associated with metabolic disorders, which carry a substantially increased risk of developing healing complications, has increased with Canada's aging population. There is therefore a clinical need for novel modalities to circumvent fracture healing complications and improve clinical outcomes. During the initial inflammatory phase of fracture healing, immune cells such as macrophages, neutrophils and mast cells play a vital role in orchestrating the molecular stimuli to initiate bone healing. Mast cells play a particularly crucial role in bone healing. Activated platelets at the fracture site release tremendous quantities of inorganic polyphosphates (polyPs) which play a role in initiating blood coagulation and are thought to modulate immune cell function. PolyP can induce the degranulation of mast cells; however, its role in the recruitment of mast remains undefined. In this study, we developed a novel polyP-loaded injectable and thermoresponsive hydrogel to provide localized immunotherapy at the fracture site. PolyP release profiles of the hydrogel show that released polyP is proportional to initial doping, and the release is sustained with a period coinciding with the inflammatory phase of fracture healing. Additionally, viscoelastic and biocompatibility tests reveal ideal elastic thermoresponsive behaviour for in-vivo implantation and an absence of cytotoxic effects. Furthermore, results suggest polyP can direct mast cell chemotaxis in a dose-dependent manner. Accordingly, this study has validated a novel immunomodulatory therapeutic strategy for testing in an in-vivo model of fracture healing. Ultimately, this bioactive hydrogel will serve to modulate the body's own immune system, enhance bone healing, improve clinical outcomes, and reduce the burden on the healthcare system.

Résumé

Les fractures font partie des blessures musculosquelettiques les plus fréquentes. Au cours des années 2015-2016, il y a eu un total de 130 000 fractures au Canada qui ont été associées à une morbidité et à des dépenses importantes pour le système de santé. Environ 5 à 10 % des patients fracturés subiront des complications telles que des non-unions. Ces complications nécessitent généralement des chirurgies de révision invasives, mais elles ne réussissent pas toujours. L'incidence des fractures associées aux troubles métaboliques qui comportent un risque considérablement accru de développer des complications qui augmentent avec le vieillissement de la population canadienne. Il existe donc un besoin clinique de nouvelles modalités pour contourner les complications de la consolidation des fractures et améliorer les résultats cliniques. Au cours de la phase inflammatoire initiale de la consolidation des fractures, les cellules immunitaires telles que les macrophages, les neutrophiles et les mastocytes sont vitaux dans l'orchestration de la consolidation osseuse. Les plaquettes activées au site de la fracture libèrent d'énormes quantités de polyphosphates inorganiques (polyP) qui jouent un rôle dans l'initiation de la coagulation sanguine et la modulation de la fonction des cellules immunitaires. PolyP peut induire la dégranulation des mastocytes, mais son rôle dans leur recrutement n’est pas encore bien défini. Dans cette étude, nous avons développé un nouvel hydrogel injectable et thermosensible chargé de polyP pour fournir une immunothérapie localisée au site de la fracture. Les profils de libération de polyP de l'hydrogel montrent que le montant de polyP libéré est proportionnel au dopage initial et que la libération est maintenue pendant une période concurrente avec la phase inflammatoire de la consolidation des fractures. De plus, des études viscoélastiques et de biocompatibilité révèlent un comportement thermosensible élastique idéal pour une implantation in-vivo et une absence d'effets cytotoxiques. En outre, les résultats suggèrent que le polyP peut diriger la chimiotaxie des mastocytes de manière dose-dépendante. En conséquence, cette étude a validé une nouvelle stratégie thérapeutique immunomodulatrice à tester dans un modèle in-vivo de guérison des fractures. En conclusion, cet hydrogel bioactif servira à moduler le système immunitaire, améliorer la consolidation osseuse, améliorer les résultats cliniques et à réduire le fardeau sur le système de la santé.

Acknowledgements

The past two years working under Dr. Rahul Gawri and Dr. Paul A. Martineau have been a great pleasure. Namely, I am grateful for their constant support and direction throughout my master's program. Dr. Gawri for your contagious passion for research, mentorship, and for always pushing me to improve and do more. Dr. Martineau for your unwavering sense of humour, and for providing me with a valuable clinical perspective of research, which will undoubtedly serve me well in my future career. I would also like to thank Dr. Xavier Banquy for his continued guidance and support and for the bi-weekly long and insightful conversations about polyP release curves.

I would like to thank my research advisory committee chair Dr. Jacques Lapointe and committee member Dr. Chan Gao for their time and thoughtful feedback. Additionally, I would like to thank the Canadian Institutes of Health Research and the Research Institute of the McGill University Health Centre for funding my thesis.

My time as a graduate student could not have been better and that was due to the numerous graduate students and post-doctoral fellows whom I was lucky enough to work alongside. Ateeque Siddique and Matthew Mannarino for showing me the ropes of cell culture and staining, and for your patience in teaching a young and eager graduate student. Jean-Gabriel Lacombe for helping make the transition to Montreal better, and for extending my hockey career. Suliman Al-Shammari for your support, and all the delicious food. Deepak Chauhan, Chang-sheng, Hu Zhang, and the rest of the Banquy lab for helping me throughout my time at the University of Montreal. To all the graduate students and technicians on C-10 at the MGH, particularly Rachad Aita, Justin Matta, Misghana Kassa, Kulsum Tai, Iris Kong, and Sanjima Pal, thank you for making science fun!

Finally, thank you to my family and friends for your love and support, and to everyone who contributed to the successful completion of my master's thesis. Your support has been instrumental in shaping my academic growth and achievements.

List of Figures and Tables

Chapter 1:

Figure 1: Study Objectives and Hypothesis

Chapter 2:

Figure 1: Chemical structure of polyP

Figure 2: Role of polyP in coagulation and hemostasis

Figure 3: Role of mast cells in fracture healing

Chapter 3:

Figure 1: Schematic of μ-Slide chemotaxis chip

Figure 2: Mast cell and macrophage trajectory plots

Figure 3: Mast cell and macrophage center of mass displacement analysis

Figure 4: Mast cell and macrophage speed of cell movement analysis

Table 1: Sol-to-gel transition analysis of tested polymers

Figure 5: PolyP release profile

Figure 6: Rheological properties of the hydrogel formulation

Figure 7: Scanning electron microscopy images of the hydrogel formulation

Figure 8: Cell viability and adhesion

Figure 9: Ex-vivo hydrogel adhesion

Abbreviations

Abbreviation	Name
ADP	Adenosine diphosphate
AIBN	Azobisisobutyronitrile
ALP	Alkaline phosphatase
AM	Acetoxymethyl
ATP	Adenosine triphosphate
bFGF	Basic fibroblasts growth factor
BMP	Bone morphogenic protein
BSP	Bone sialoprotein
CMC	Critical micelle concentration
COL-1	Collagen Type I
Cpa3	Carboxypeptidase A3
Cre	Cyclization recombinase
CXCL1	C-X-C motif chemokine ligand 1
DAMP	Damage-associated molecular pattern
DAPI	4’,6-diamino-2-phenylindole
DMEM	Dulbecco’s modified essential medium
EGF	Epidermal growth factor
ESI-MS	Electrospray ionization mass spectrometry
FBS	Fetal bovine serum
FGF	Fibroblast growth factor
G’	Storage modulus (elastic)

G”	Loss modulus (viscous)
GF	Growth factor
H.BMMSC	Human bone marrow mesenchymal stem cell
hAT-MSCs	Human adipose tissue-derived mesenchymal stem cells
hBM	Human bone marrow
HCL	Hydrochloric acid
IGF	Insulin-like growth factor
IL-1	Interleukin-1
IL-6	Interleukin-6
Kit	Receptor tyrosine kinase
MEMα	Minimum essential medium alpha
MMP-13	Matrix metalloproteinase-13
MPA	3-mercaptopropionic acid
MSC	Mesenchymal Stromal Cells
MWCO	Molecular weight cut-off
NF-κB	Nuclear factor kappa-light-chain enhancer
NVCL	N-Vinyl caprolactam
OC	Osteocalcin
OPG	Osteoprotegerin
OPN	Osteopontin
OSX	Osterix
P-NMR	Phosphate nuclear magnetic resonance

P2Y1	Purinergic receptor P2Y, G-protein coupled 1
PBS	Phosphate buffered saline
PDGF	Platelet-derived growth factor
PEO	Polyethylene oxide
P_i	Inorganic phosphate
PLC	Phospholipase C
PNVCL	Poly-N-vinyl caprolactone
polyP	Inorganic polyphosphate
POSS	Polyhedral oligomeric silsesquioxane
PPK	Polyphosphate kinase
PPK1	Polyphosphate kinase 1
PPK2	Polyphosphate kinase 2
PPO	Polypropylene oxide
PRP	Platelet-rich plasma
RBL	Rat basophilic leukemia
RPMI	Roswell Park Memorial Institute
Runx2	Runt-related transcription factor
SCF	Stem cell factor
SEM	Scanning electron microscopy
Sox9	SRY-box transcription factor 9
STP	Standard tissue culture plastic
TNF	Tumour necrosis factor
VEGF	Vascular endothelium growth factor

Author Contribution

The following thesis is written in a manuscript-based format complying with the requirements of the thesis guidelines as outlined by McGill University's Graduate and Postdoctoral Studies Office (GPSO). A comprehensive review of the literature for this research is included in Chapter 2. The original experimental work is presented in Chapter 3 and is formatted as a manuscript in preparation for submission. The data presented in Chapter 3 is part of this manuscript-based thesis only and no other thesis will use this data. Experiments, data collection, and analysis were performed by the author with the help of co-authors. The author wrote the manuscript, designed some experiments, and generated the figures under the direction of his supervisors. Co-author contributions to the experimental work are outlined below.

Rayan Ben Letaifa developed the hydrogel formulation, performed drug release studies, and characterized the hydrogel. Rayan also performed all tissue culture, biocompatibility studies, immune cell chemotaxis studies, statistical analysis and wrote the manuscript.

Deepak S. Chauhan mentored the author and helped with hydrogel development and testing, and with characterization using scanning electron microscopy.

Chang-sheng Wang provided his expertise in materials engineering and taught and helped perform rheological analysis of the hydrogels.

Hu Zhang synthesized hydrogel chitosan-g-PNVCL and provided expertise in material preparation for scanning electron microscopy.

Paul A. Martineau provided lab space and contributed to the conception of the study. Dr. Martineau mentored the author, co-supervised the entire thesis work, and helped prepare the manuscript.

Xavier Banquy provided lab space, provided materials, and oversaw experimental procedures. Dr. Banquy mentored the author, provided supervision in the thesis, and helped prepare the manuscript.

Rahul Gawri secured funding, provided lab space, materials, and oversaw experimental procedures. Dr. Gawri mentored the author, supervised the entire thesis from conception to reality, and helped prepare the manuscript.

Chapter 1 : Introduction

Over the course of our lifetimes, many of us have fractured a bone or know someone who has. While the vast majority of fractures heal properly, approximately 1 in 10 fractures will result in a fracture complication such as a non-union, mal-union, or delayed union [1]. The rate of fracture complications is further exacerbated in patients suffering from chronic and metabolic disorders such as osteoporosis and diabetes [2]. The impact of these fractures on patients and the health care system is tremendous, and warrants investigations into new therapeutic alternatives to help prevent such complications, given the increased prevalence of metabolic disorders amongst the ageing Canadian population [3].

Osteoimmunology is a rapidly growing interdisciplinary field of research studying the key molecular players involved in the highly ordered sequence of cell interactions leading to fracture healing [4]. The optimal treatment for complex fractures and large bone defects remains a significant unresolved issue in orthopaedics and osteoimmunology alike. Healing can be broadly described by three overarching phases: the inflammatory, repair, and remodelling phases. Downstream fracture healing is highly dependent upon the initial inflammatory phase, which is orchestrated by the local and systemic responses to injury, and inter-cellular crosstalk between various immune cells and mesenchymal stromal cells. Disruption to this inter-cellular communication, or dysregulation of acute and chronic inflammatory processes can directly lead to impaired fracture healing [5]. Recently, as the critical function of immune cells in fracture healing has become better understood, numerous studies have focused on the potential of immunomodulation as a strategy to accelerate fracture healing, and prevent impaired fracture healing [6].

Currently, bone grafts and recombinant growth factors, which can cause considerable morbidity on their own, are used in a significant proportion of cases in North America to promote bone healing in patients at risk of non-union [7]. Accordingly, localized immunotherapy could prove to be a safer and more cost-effective solution to promoting bone repair.

Mast cells, known for their role in pathological conditions, are critical regulators of the initial inflammation comprising the inflammatory phase of fracture healing, and play a role throughout the rest of the process. They migrate to and mature at the fracture site to aid in bone and soft tissue repair [8]. Previous work by our group has demonstrated that mast cell-deficient mice developed fibrous non-unions [9] associated with highly disorganized healing, and impaired neo-vascularization [10]. Taken together with their wide range of pro-osteogenic growth factors, cytokines, and chemokines, mast cells represent a potential immunotherapeutic target in assisted fracture healing.

Inorganic polyphosphates (polyP), a little known but tremendously important innate molecule, plays an important role in eliciting pro-inflammatory cascades at the fracture site [11], and modulating gene expression in a wide variety of cell types [12]. Furthermore, polyP has been shown to have osteogenic effects on mesenchymal stem cells and osteoblasts alike [12]. A recent study identified polyP as a regulator of pro-inflammatory mast cell function [13]. At the fracture site, polyP released from degranulating platelets is thought to play a role as a transductor in recruiting immune cells during the inflammatory phase; however, its role in recruiting mast cells has yet to be characterized. Accordingly, this thesis work aims to characterize the immuno-tactic effects of polyP on mast cells and develop a thermoresponsive and injectable polyP-loaded hydrogel for the purpose of delivering localized immunotherapy at the fracture site. Ultimately, this body of research is founded on the global hypothesis that polyP plays a crucial role in the

initial orchestration of inflammatory events and that mast cells are pivotal to the recruitment and coordination of immune, skeletal, and vascular activity at the fracture site. From a clinical standpoint, this project attempts to generate a novel drug delivery system serving to modulate the body's own immune system, enhance bone healing, improve clinical outcomes, and reduce clinical strain.

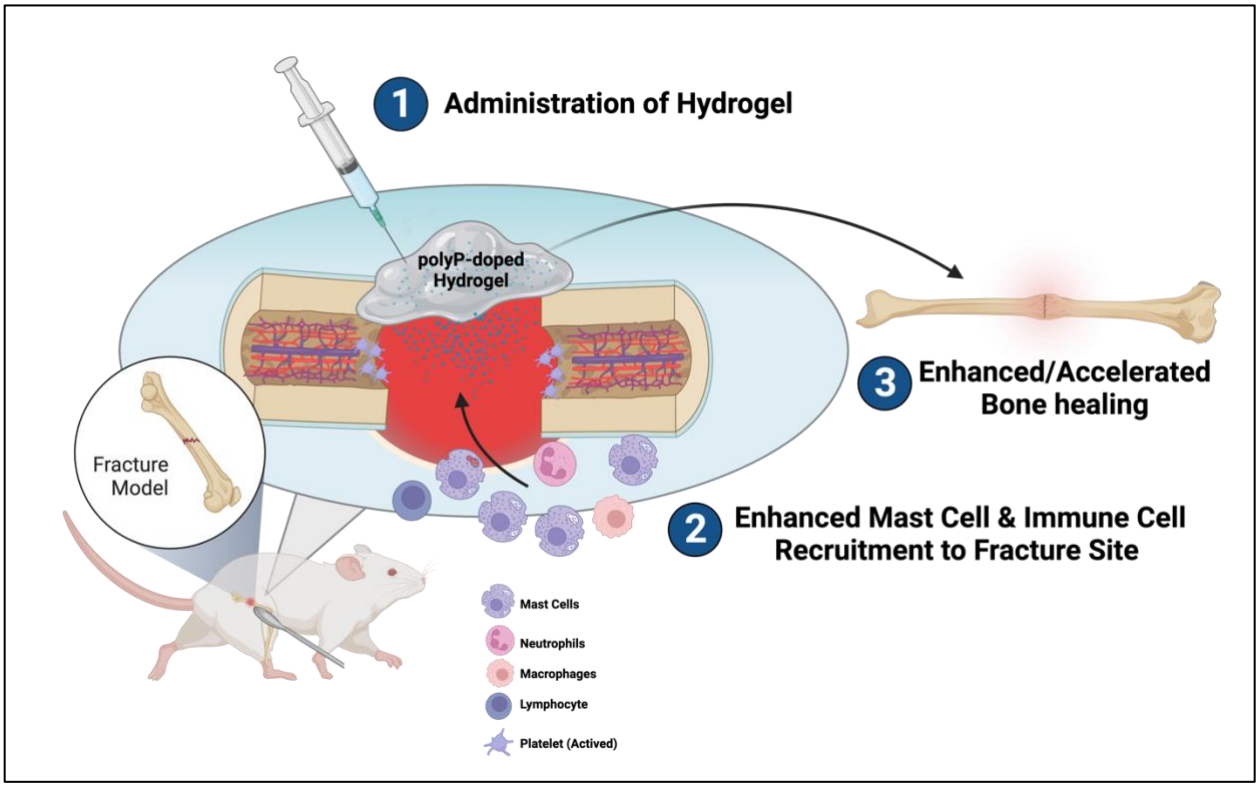

Figure 1: The overarching hypothesis of this thesis is that by developing a polyP-releasing hydrogel that can be implanted at the fracture site, enhanced mast cell and immune recruitment will ensue and therefore fracture healing can be enhanced and accelerated. This could be achieved by an ensuing increased concentration of pro-osteogenic growth factors and cytokines at the fracture site. Created with Biorender.com

Chapter 2: Literature Review

2.1 Inorganic Polyphosphates

Inorganic polyphosphates (polyP) are linear chains or orthophosphate residues linked by high-energy phosphoanhydride bonds, in a similar fashion to adenosine triphosphate (ATP). Although it bodes a relatively simple chemical structure, it is ubiquitous in both simple and complex organisms across all forms of life. Furthermore, its structure varies greatly between different organisms. Bacteria typically produce long-chain polyP that can include more than 1000 phosphate subunits and are often located in dense electronegative granules called acidocalcisomes [14, 15]. In contrast, eukaryotic cells produce shorter-chain polyP that typically comprise a range of 80 – 200 phosphate subunits [16]. PolyP plays a wide variety of roles in homeostatic, inflammatory, and metabolic processes as outlined below. As we begin to uncover many of its important functions in higher eukaryotes, we continue to lack a thorough understanding of polyP biogenesis and its mechanism of action; however, its significance in physiology has generated substantial interest in polyP research.

2.1.1. Origin and Evolutionary Role

The abundance and universality of polyP in all domains of life make it an intriguing molecule from an evolutionary perspective. Generated by dehydration of orthophosphate residues, polyP could be found in volcanic condensates and deep oceanic steam vents [17]. Its role as a biomolecule has only been recently discovered. In prokaryotes, null mutants of a key polyP synthesizing enzyme, polyphosphate kinase 1 (PPK1), produced extremely low levels of polyP and were unable to survive [18, 19]. Furthermore, these cells had an appreciable defect in quorum sensing, virulence, and biofilm formation, suggesting an important role for polyP in bacterial

pathogenesis [20]. Interestingly, polyP also appears to have an upstream regulatory effect. Due to its structure, polyP has a high affinity to histone-like proteins, enabling it to displace them from their attachment to the DNA-nucleoid complex [21]. This finding suggests polyP has a role to play in epigenetic control of gene expression. A study investigating the role of polyP in a *D. discoideum* null mutant of PPK1 found this organism to be significantly deficient in growth and sporulation; however, significant levels of polyP were retained inside vacuoles called "acidocalcisomes", which was mainly attributed to the function of polyphosphate kinase 2 (PPK2) [20]. These acidocalcisomes are calcium and polyP-rich, are accountable for calcium fluxes, and are conserved from bacteria to humans [22]. The conservation of these vacuoles in higher eukaryotes suggests an important evolutionary role for polyP.

2.1.2. Chemical Structure

The chemical structure of polyP consists of tetrahedral orthophosphate residues, linked by high-energy phosphoanhydride bonds, forming inorganic chains with a highly flexible backbone. Due to its negatively charged oxygen atoms, polyP is highly anionic. Due to its anionic properties, it can chelate a wide range of cations as well as sequester toxic metals including mercury and cadmium. Moreover, due to its flexibility, it can be localized in the cell in a variety of orientations, and in a relatively stable form to play a wide variety of roles.

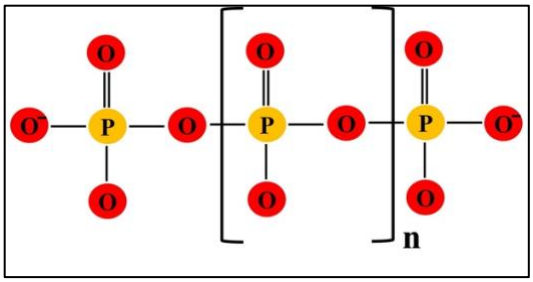

Figure 1: Chemical structure of inorganic polyphosphates. 'n' signifies the number of linked PO_4 subunits.

2.1.3. Multifunctional Role in Biology

PolyP is a widely multifunctional molecule in biology, in a wide array of organisms. Due to its non-toxic nature, polyP is frequently added as a nutritive food additive [23], an antioxidant [24], and a chelator of multiple divalent cations [25]. When found at chain lengths of less than 100 orthophosphate residues, polyP is water-soluble [26]. Over the years as polyP has gauged increasing interest, it has been demonstrated that polyP acts as an energy storage molecule, as a donor for sugars and adenylate kinase, an inducer of apoptosis, and has been shown to play a role in the mineralization of bony tissue [27]. Upon the discovery that platelets contain abundant levels of polyP in their dense granules, a role was demonstrated for polyP in blood coagulation, fibrinolysis, and inflammation [11]. Moreover, polyP has been shown to play a role in modulating the expression of many important genes for bone formation. Its role in physiology is extensive and is just now being uncovered. In this review, the role of polyP in bone and cartilage formation will be discussed in greater depth.

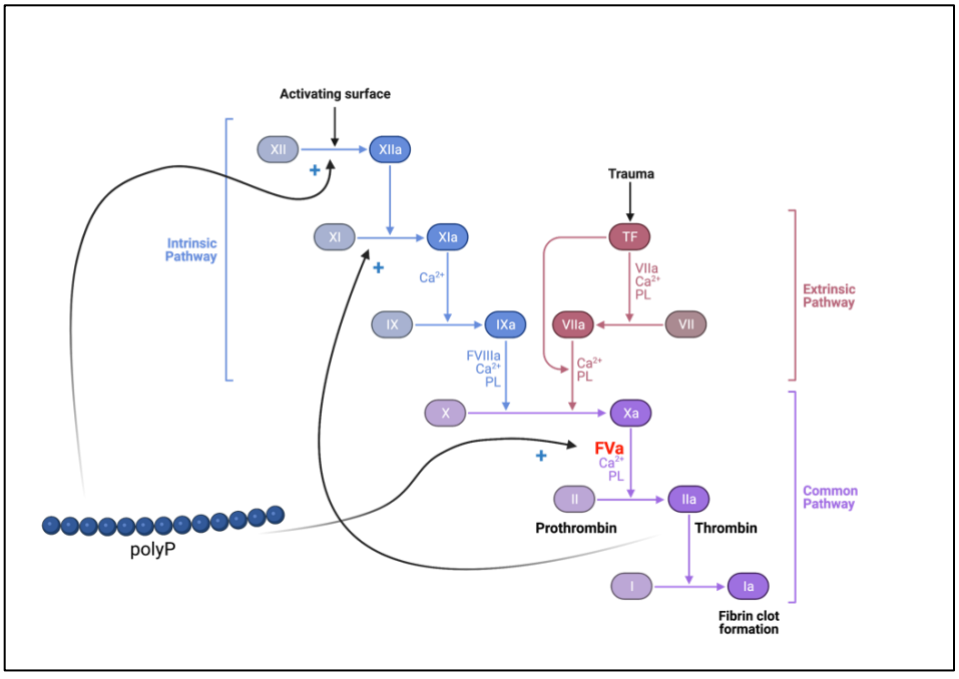

Figure 2: Upon platelet activation, polyP is secreted and contributes to hemostasis. PolyP can act at several points in the clotting cascade. PolyP can activate Factor V [28], stimulate the activation of Factor XI by thrombin [29], and activate Factor XII to Factor XIIa through the intrinsic pathway [30]. Created with Biorender.com.

As previously mentioned, polyP biosynthesis has been widely studied in microorganisms, but its synthesis in higher eukaryotes remains unknown. They are most often found in intracellular organelles described as "acidocalcisomes" due to their acidity, and their substantial calcium ion content [31]. With regards to mammalian cells, acidocalcisomes are major components identified in dense granules [22], and are found in the inflammatory subset of mast cell secretory granules [13].

2.1.4. Applications of polyP in bone and cartilage regeneration

Critical functions for polyP have been identified in coagulation, inflammation, and bone and cartilage regeneration. Concerning bone regeneration, polyP may promote osteoblast differentiation, initiate calcification, and inhibit the activity of osteoclasts [27]. As such, polyP has been highly touted as a candidate in biomaterial applications in cartilage and bone regeneration.

Mesenchymal stromal cells (MSCs), a type of stem cell primarily found in connective tissues, are highly proliferative cells capable of differentiating into chondrocytes, osteoblasts, muscle cells, and adipocytes [32]. PolyP can drive the osteogenic differentiation of mesenchymal stem cells (MSCs) by upregulating the expression of several osteogenic transcription factors including Runx2 and Sox9 [33]. Moreover, polyP initiates the Fibroblast growth factor 23 (FGF23) signalling pathway to induce proliferation and osteogenic differentiation of MSCs via upregulation

of osteopontin (OPN), osteocalcin (OC), and Osteoprotegerin (OPG) expression [34]. A study conducted by Wang *et al.* [35] revealed that polyP could promote both osteogenesis and chondrogenesis; however, this activity could only be observed in MSCs that were cultured in osteogenic or chondrogenic media. Following osteogenic stimulation, polyP has the ability to enhance the expression of BMP-2, ALP, collagen type I (COL-1) and COL-2. MSCs cultured without osteogenic induction did not demonstrate positive staining with alizarin red S after the addition of polyP, and there was no evidence of cell mineralization [35]. Recently, a study performed by Gawri *et al.* showed that the anabolic effect of polyP is mediated by calcium signalling and that the effect was highly dose and chain length-dependent [36].

Research into the applications of polyP in bone and cartilage regeneration is fast emerging and shows tremendous promise. Given the current burden of bone and cartilage morbidity, further translational research will play an important role in bone and cartilage tissue engineering for years to come.

2.1.5. Quantification of inorganic polyphosphates in the life sciences

Given its increasingly important physiological role, developing methods for the analysis of polyP in the life sciences is paramount to overcoming current analytical barriers. Six measuring metrics are relevant to polyP research; these include molecular structure, average chain length, chain length distribution, cellular localization, cation composition, and concentration. For the purpose of this study in which drug delivery is the objective, the scope of this review will focus on quantitative methods for analyzing polyP release.

Metachromacy refers to the alterations of a dye's absorbance spectrum when it attaches to a specific substance. This property can be used to detect polyP with certain dyes including methylene blue, and toluidine blue O, among others. For example, toluidine blue decreases the

absorption wavelength from 630 nm to 530 nm [37]. Fluorescent dyes such as 4',6-diamino-2-phenylindole (DAPI), JC-D7, and JC-D8 show minimal fluorescence when freely dissolved, but their fluorescence increases greatly when bound to polyP. When DAPI is bound to DNA, a blue-white complex is formed; however, when it is bound to polyP, a yellow-green complex is formed. This detection of polyP is achieved by both an increase in the fluorescence and a shift in the emission spectrum [38]. This method has been utilized to quantify polyP in mammalian tissues [39]. Nonetheless, this method has limitations including the presence of lipid inclusions [40], nucleotides [41], and inositol phosphates [42] interfering with fluorescence readings.

Because of their high specificity for polyP, enzymatic assays are also a popular tool for quantifying polyP. These types of assays are typically unaffected by common impurities and only necessitate readily available laboratory equipment. Two enzymatic assays are most prominent concerning polyP quantification: the PPK enzyme assay, and the Christ *et al*. assay. In the polyP kinase (PPK) assay, an inorganic phosphate (P_i) group is transferred from polyP onto adenosine diphosphate (ADP) and then is quantified with a standard firefly luciferase assay. This assay quantifies the total polyP concentration and is sensitive down to picomolar concentrations of polyP. The Christ *et al*. assay, on the other hand, not only quantifies the total polyP concentration but also the polyP chain length [43]. This assay includes the hydrolysis of polyP with *Saccharomyces cerevisiae* exophosphatase 1 and *S. cerevisiae* inorganic pyrophosphatase 1 into P_i, and subsequently assayed with a single reagent colorimetric detection. Overall, this enzymatic assay comprises several consecutive enzymatic steps that have potential for high-throughput detection, but the method is better suited for shorter polyP chains.

Phosphate nuclear magnetic resonance (P-NMR) is a powerful tool for the characterization and quantification of polyP. P-NMR can distinguish all phosphate nuclei with differing electronic

environments, and therefore their unique electromagnetic shielding. To this extent, the varying chemical shift allows this technique to characterize total polyP concentration, average chain length, and distribution of chain length with high specificity. Although this technique can reveal a great deal of information about a large quantity of polyP, samples with a low polyP concentration cannot be evaluated.

Chromatography facilitates the separation of substances based on the differential distribution of their constituents between the stationary phase and a mobile phase. Because chromatography typically employs a UV or visible light detector to quantify the molecule, a UV-absorbing or visible light chromophore must be affixed onto the molecule if it cannot be detected in these regions. PolyP cannot be detected in these regions, and as such requires the grafting of a chromophore, or an automatic flow injection system with a post-column derivatization [44]. The most commonly applied method for freely dissolved polyP of chain lengths less than 50 subunits is ion-exchange chromatography [45, 46]. The sensitivity of this method is great for chain lengths of less than 10 subunits, whereas the peaks of chains with 10-50 subunits typically overlap with separation based on chain length. Although this method is great for the separation of polyP from other constituents, assuming the absence of other polyanions, its detection for quantification of total polyP concentration requires more sensitive detection methods [44].

Electrospray ionization mass spectrometry (ESI-MS) is another powerful tool that can detect polyP concentrations with great sensitivity, typically in the range of 10 nM to 100 μM [47]. This method is advantageous because it explicitly detects polyP by mass and does so in a quick and high-throughput manner without requiring UV-absorbing chromophores. Thus far, however, this method has only been used to detect polyP chains of up to 4 subunits. Further method

development utilizing ESI-MS for the detection of longer-chain polyP would permit improved polyP quantification with greater sensitivity for a broader range of applications.

Many other methods are also available such as other types of chromatography, electrophoresis, and quantification of the polyP counterion. The recurring with all polyP quantification methods is that sensitivity is particularly high with shorter chain lengths, but not as high with longer chain lengths. Given the discovery of the physiological importance of longer chain length polyP, better methods for their quantification will need to be developed.

2.2. Fracture Healing

A bone fracture occurs when the continuity of a bone is broken due to physical force, tension, or trauma. There are different types of fractures, and they can range from small hairline fractures to complete separation into two or more fragments. Fractures can occur in any bone in the body and can be caused by a variety of reasons including falls, accidents, repetitive stress, sports injuries, and certain conditions that weaken bones [48, 49]. Fracture healing comprises a series of complex biological responses to repair the fractured bone in order to regain its functional and structural integrity.

2.2.1. Stages of fracture healing

As previously described, the restoration of the structural and functional integrity of a fractured bone is a complex physiological process involving a series of meticulously orchestrated phases [50]. These phases are outlined as follows:

1) Hematoma formation and inflammation phase: shortly after a fracture occurs, disruption of blood vessels causes haemorrhage and the subsequent formation of a peri-fracture hematoma [51]. This hematoma functions as an infiltration site for immune cells where the inflammatory response is initiated [52]. Neutrophils and macrophages are recruited to the fracture site, where

they attempt to eliminate cellular debris and foreign particles [53, 54]. This inflammatory phase is characterized by high cellular activity and cytokine release, thereby establishing the foundation for subsequent healing phases [55, 56].

2) Soft callus formation: as a result of the inflammatory environment, MSCs and fibroblasts infiltrate the fractured area and contribute to the formation of a soft callus [57-59]. This fibrous matrix, mainly composed of collagen and fibronectin, provides initial stability by bridging fractured fragments [60]. Chondrocytes, which are derived from MSCs, produce hyaline cartilage, working to strengthen the provisional union [61].
3) Hard callus formation: in the following weeks, the chondrocytes within the soft callus differentiate into osteoblasts, which are primarily responsible for the formation of bone [62]. This change and synthesis of collagen type X promotes the mineralization of cartilaginous callus, resulting in the formation of woven bone [63, 64]. Although not as resilient as mature bone, this hard callus provides adequate mechanical stability at the fracture site [65, 66].
4) Remodelling phase: beginning weeks to months post-injury, the hard callus undergoes significant remodelling [67]. Osteoclasts begin resorbing excess bony tissue, thereby facilitating the reshaping of the callus and the restoration of the original anatomical shape [68]. Additionally, osteoblasts produce lamellar bone, which is characterized by increased strength and durability [69].
5) Mature bone formation: the culmination of fracture healing is represented by the transformation of remodelled bone into mature and compact lamellar bone which resembles the original bone. Further bone turnover by osteoblasts and osteoclasts produces biomechanical characteristics equivalent to those of a healthy bone, ultimately resulting in the restoration of bone integrity [70].

Fracture healing may be affected by a variety of factors, including the type and location of the fracture, the age of the patient, their general health, and the therapeutic intervention undertaken. Minimizing fracture complications involves a comprehensive approach and understanding of the distinct yet intertwined stages.

Fracture healing can be further characterized as primary, direct healing, secondary, or indirect healing. Primary and secondary healing comprise distinct mechanisms with respect to their biological processes, conditions required for healing, and timelines. Primary fracture healing takes place when the fractured ends are perfectly aligned and do not move apart. At the microscopic level, lamellar and Haversian canals are directly remodelled during the healing process [71]. Complete stability is necessary with the ends of the bones being rigidly fixed, where the cortex of one side of the fracture end must be connected to the cortex of the opposing fractured end in order to restore physical continuity of the bone [72]. This is typically accomplished through internal fixation with the use of rods, screws, and plates. Because this type of healing is reliant on perfect anatomical alignment and rigid fixation, any movement between bone fragments can disrupt this process and result in healing complications. Osteons mature into lamellar bone through remodelling, which results in the fracture site mending without the development of a callus or significant inflammation [73]. Due to the direct bone remodelling mechanism, primary bone healing is usually faster than secondary healing and involves a quicker restoration of the bone's original structure.

Secondary bone healing takes place when some degree of movement or gap between the fracture bony ends is present. This is the more common type of bone healing and consists of both intramembranous and endochondral ossification as outlined in the stages above. The healing

begins with the formation of a blood clot and eventual soft callus made of fibrous cartilaginous tissue at the fracture site [74]. The cellular response is heavily influenced by inflammatory immune cells during early stages and dominated by fibroblasts, chondrocytes, and osteoblasts in the latter stages [57]. Compared to primary healing, secondary healing is a longer process as callus formation and remodelling can take several weeks to months prior to full mechanical restoration of the bone [67].

2.2.2. The role of immune cells in fracture healing

Recent advances in immunology have uncovered the intricate role of immune cells in tissue repair processes. Osteoimmunology is the interdisciplinary field studying the molecular interplay between the skeletal system and the immune system [75]. This field of study has gained immense attention over recent years and provides insights into how fracture healing can be enhanced through immunomodulation [76]. Immune cells such as macrophages, neutrophils, T cells, regulatory T cells, and mast cells actively contribute to inflammation, angiogenesis, chondrogenesis, and osteogenesis in the process of fracture healing [77].

The infiltration of neutrophils and macrophages at the fracture site defines the initial inflammatory phase [78]. By releasing cytokines and reactive oxygen species, neutrophils initiate the inflammatory cascade [79]. Both pro-inflammatory (M1) and anti-inflammatory (M2) macrophages dynamically modulate the transition from inflammation to tissue repair [80]. M1 macrophages secrete pro-inflammatory mediators which promote angiogenesis and further cellular recruitment, and M2 macrophage-derived mediators contribute to the resolution of inflammation and the beginning of tissue regeneration [81, 82].

Angiogenesis is essential for fracture healing in order to ensure oxygen and nutrient delivery to the fracture site [83]. Immune cells, particularly mast cells, macrophages, and T cells,

secrete pro-angiogenic factors such as vascular endothelium growth factor (VEGF) and fibroblast growth factor (FGF), which promote the development of new vessels [84]. In addition, immune cells contribute to the formation of a soft callus, helping to stabilize the fracture site [85].

Osteogenesis, which involves the differentiation of MSCs into osteoblasts, is the hallmark of fracture healing. Immune cells, specifically T cells and regulatory T cells, regulate osteoblast differentiation and bone deposition by secreting osteogenic factors [86] and modulating osteoclast activity [87, 88]. Furthermore, T cells influence the equilibrium between bone resorption and formation during bone remodelling [89].

Recent evidence indicates that immunomodulation may have therapeutic potential for fracture healing. Measures targeting immune cell polarization, cytokine release, and immunomodulatory molecules may accelerate and enhance the healing process. Immunotherapeutic interventions that leverage the regenerative capacity of certain immune cells, such as macrophage-based therapies, have the potential to advance fracture healing techniques [90, 91]. Mast cells also play an important role in fracture healing and have also been investigated as fracture healing immunotherapy candidates by our group. Below is an overview of their role in bone repair.

Mast cells, best known for their involvement in allergic reactions, are tissue-resident immune cells and are involved in a wide array of physiological processes. Mast cells are distinct within the immune cells due to their large electron-dense secretory granules. These secretory granules contain a broad range of pre-formed mediators required for optimal fracture healing, including biologically active amines (e.g., histamine), heparin, pro-inflammatory cytokines (e.g., interleukin-6 (IL-6), interleukin-1 (IL-1), tumour necrosis factor (TNF)), and growth factors (e.g., FGF, VEGF) [92]. Because mast cell progenitors mature based on the local microenvironment

[93], the mediators found in their granules vary depending on the tissue [94-96]. Although the number of mast cells is few in the bone marrow, epiphysis, and diaphysis, they are found in greater numbers in the metaphyseal bone marrow where most of the bone remodelling takes place [8]. Their proximity to the site of bone remodelling, along with its wide range of pro-osteogenic growth factors and cytokines, suggest an important role for mast cells in bone physiology. During initial events at the fracture site, mast cells play a critical role in regulating fracture-induced inflammation, mainly by releasing IL-6, and influencing innate immune cell recruitment [97]. Previously, we have shown in a murine model of unicortical window defect of mast cell-deficient $Kit^{W\text{-}sh/W\text{-}sh}$ mice that healing was delayed due to compromised replacement of woven bone with compact bone and associated impaired re-vascularization [9]. Additionally, in a c-kit independent $Cpa3^{Cre/+}$ model, bone healing was also impaired as demonstrated by decreased cortical bridging, bone mineralization, and vascularization [10]. Another group showed that in the absence of mast cells, levels of pro-inflammatory cytokines IL-6, IL-1β, and chemokine CXCL1 were significantly reduced and that the recruitment of neutrophils and macrophages to the fracture site was also impaired [98]. Taken together with their ability to ability to respond to specific stimuli [99, 100], their significant involvement in early fracture healing identifies mast cells as potential targets for immunotherapy in assisted bone repair.

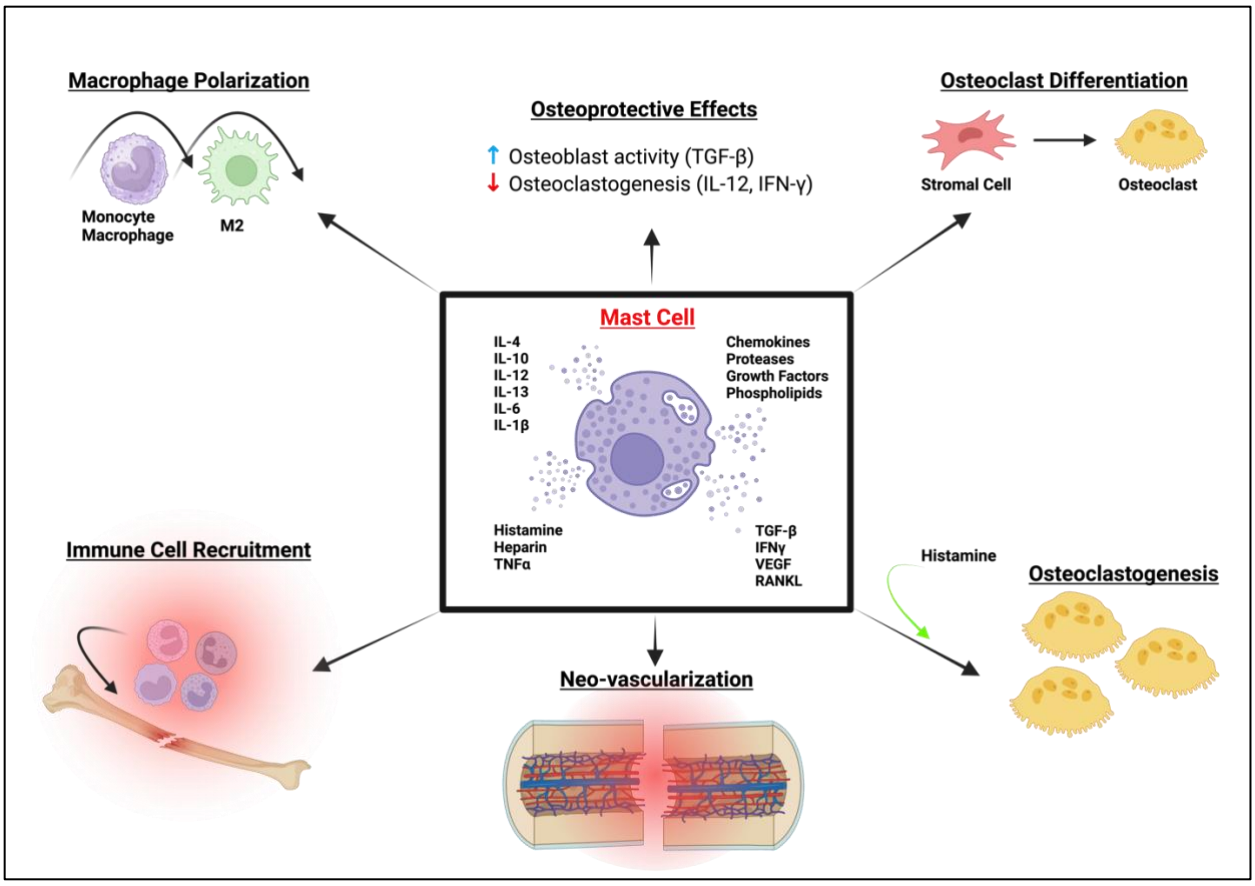

Figure 3: Outline of the documented roles of mast cells in fracture healing. Mast cells play an osteoprotective by promoting osteoblast and inhibiting osteoclast activity through TGF-β, IL-12 and IFN-γ, respectively [101, 102]. Furthermore, mast cells may influence macrophage polarization and immune cell recruitment to the fracture site through a variety of pro-inflammatory cytokines [103]. Additionally, mast cells play a significant role in neo-vascularization, mainly through stored VEGF [104]. Finally, through histamine stored in its granules, they can also stimulate osteoclastogenesis [105]. Created with Biorender.com.

2.2.3. Fracture complications

Fracture repair is usually successful, however, approximately 5-10% of fracture patients will experience complications such as malunions, delayed unions, or non-unions [49]. In the

United States (US), direct and indirect costs during the first six months post-trauma are estimated to be $23,000.00 per individual fractured limb [106]. Fractures of long bones such as the tibia or the femur are particularly difficult to manage, and the risk of complications contributes significantly to reduced quality of life and post-trauma disability [107]. Frequent causes of non-union and malunion include infection, inadequate bone fixation, poor blood supply, and activities that hinder bone healing such as smoking and alcohol abuse [2]. Fractures endured in high-energy trauma and associated with significant soft tissue damage, such as open fractures, are particularly susceptible to non-union [108, 109]. Patients with chronic diseases such as diabetes, osteoporosis, obesity, malnutrition or neuropathy also have an increased baseline risk for non-union [110].

2.2.4. Fracture management and treatment

The treatment for non-healing bone injuries can be challenging and requires a comprehensive approach. Many non-unions will require corrective revision surgeries, and these can sometimes be unsuccessful [2, 111, 112]. Surgical treatment of these complications typically includes implantation of autologous or non-autologous bone grafts, debridement, electrical stimulation, or biological enhancement therapy such as percutaneous injection of bone marrow [113], or bone morphogenic protein (BMP) [114, 115]. Although the use of BMP initially showed promise, it brings along a set of distinct issues including high cost of treatment, unintended bone growth, inflammatory complications, and infection [116-118]. As such, novel therapeutic approaches are required in order to aid in circumventing fracture complications.

2.3. Hydrogels

Hydrogels are three-dimensional networks of polymers that can absorb and retain large quantities of water. Due to their remarkable properties such as high-water content, mechanical strength, and

biocompatibility, they have a wide range of applications that span many disciplines. The polymers composing hydrogels can be derived from natural sources or synthesized. These polymers are hydrophilic in nature, and when encountering water, they can absorb water and thereby swell. The swelled interlinked polymers are what constitute the hydrogel [119].

2.3.1. Hydrogels for Drug Release

Hydrogels are increasingly being investigated as local drug delivery vehicles owing to their adaptable characteristics, controllable degradation, and capacity to protect labile pharmaceuticals [120, 121]. Several key benefits make hydrogels ideal for the controlled release of drugs into the body. Hydrogels are comprised of polymers that are compatible with biological systems, meaning they generally do not trigger immune responses or other adverse reactions, including cytotoxicity [122]. Their porous structure allows for gradual and sustained release over periods that can be optimized [123]. This can aid in reducing the frequency of dosing and improving the efficacy of treatment by counteracting elimination and metabolism of the drug at the site [124]. By controlling the release of the drug, the risk of toxicity can be minimized by reducing the amount of drug delivered [125]. Furthermore, the hydrogel can be constructed to target specific tissues in the body, increasing the likelihood of successful integration and retention of the hydrogel [126]. In addition, the solubility, stability, and penetration into tissues can be enhanced by using hydrogels as vehicles, rendering a more efficient therapeutic action [127]. Overall, their versatility in the context of drug delivery makes them an exciting tool for the development of new treatment modalities.

2.3.2. Mechanisms of network formation

In consideration of the therapeutic use and chemical characteristics of the polymers, numerous mechanisms can be employed in the network formation of hydrogels. Two of the most common mechanisms are chemical cross-linking and physical gelation.

Chemical cross-linking is the most common method of hydrogel formation [128]. This method involves creating a three-dimensional network by interlinking polymer chains via covalent bonds. Chemical cross-linking can be achieved by cross-linking agents. Typically, polymer chains containing reactive functional groups (such as acrylate or methacrylate groups) can be combined with cross-linking agents (i.e., cross-linkers) containing two or more reactive sites. The reactive groups on the polymer chains and the cross-linker molecule form covalent bonds upon activation, resulting in the formation of a stable network [129]. The polymerization process can be initiated by heat, light, catalysts or other chemical agents [130]. Some hydrogel networks can be formed via physical interactions, including hydrogen bonding, ionic interactions, and van der Waals forces [131]. These interactions generate reversible cross-links that permit the hydrogel to expand and contract in response to environmental variations such as temperature and pH [126]. In contrast to chemical cross-linking, physical gelation does not involve chemical reactions and instead relies on intermolecular forces between polymer chains. This type of network formation is often observed in hydrogels comprising biopolymers including agarose and alginate [132, 133]. Physical gelation can be advantageous as it does not require the use of potentially toxic chemical cross-linkers; however, they often cannot afford the same mechanical properties as chemically cross-linked hydrogels [134]. Furthermore, physical hydrogels often do not exhibit the same stability and durability profile but exhibit environmentally responsive behaviour and can more easily be tuned [135]. Accordingly, the choice of network formation will depend on the desired application and properties of the hydrogel.

2.3.3. Hydrogels for fracture healing applications

As previously mentioned, hydrogels have shown promise in a variety of biomedical applications, including fracture healing. Several properties of hydrogels make them ideal for fracture healing, and they have been employed for a variety of purposes [136]. Hydrogels can transport bioactive molecules such as growth factors and cytokines, acting as drug delivery vehicles by releasing these factors at the fracture site, and thereby enhancing the body's own healing process [137-140]. Hydrogels can also serve as a scaffold for cell growth where they can facilitate the growth and proliferation of osteoblasts and MSCs [141, 142]. In this instance, they can promote the adhesion, migration, and differentiation of cells, thereby contributing to the formation of new bone tissue [143]. These are often referred to as bone matrix mimetics [120]. Biodegradable hydrogels can degrade progressively throughout bone healing, and as the hydrogel degrades, space is created for growing bone tissue, and ultimately is supplanted by new bone [144]. Some hydrogels possess tough mechanical properties and thus can provide the mechanical support needed to reduce the risk of further damage to surrounding tissue and enhance the healing process [145]. Additionally, some hydrogel formulations are injectable or can be applied in a minimally invasive manner, allowing them to be applied in difficult-to-reach areas and potentially aiding patients for whom surgery is not indicated [146]. Despite the outlined potential benefits of these hydrogels for fracture healing, research in this area is still ongoing and their clinical use has yet to be implemented [136].

2.3.4. Poloxamer and Gellan gum-based hydrogels

Poloxamers, also referred to as Pluronics, are non-ionic surfactants and tri-block co-polymers that have undergone extensive research and application within the pharmaceutical and

biomedical domains. These applications include a wide range of functions, notably drug delivery systems [147]. Poloxamers are amphiphilic molecules comprised of hydrophilic poly(ethylene oxide) (PEO) blocks and hydrophobic poly(propylene oxide) (PPO) blocks and are able to form micelles in an aqueous environment when maintained at a concentration above a particular threshold, referred to as the critical micelle concentration (CMC) [148]. Combined with their ability to undergo sol-to-gel transition at physiological temperatures [149], poloxamers show potential for effective administration of polyP in the context of bone tissue regeneration.

Gellan gum is a water-soluble complex polysaccharide and commonly used in the food industry, and more recently for tissue engineering purposes [150-153]. Gellan gum originates from the bacterium *Sphingomonas elodea* and bodes many characteristics that make it suitable for biomedical applications [154]. Key characteristics of Gellan gum include thickening properties, stability, and synergistic properties [155]. Gellan gum can readily form gels at concentrations as low as 0.1-1%, forming a smooth transparent gel structure [156]. Moreover, Gellan gum is resistant to pH changes, enzymatic activity and heat, making it suitable for use in particularly harsh environments [157]. Finally, Gellan gum works well in synergy with other polymers as a gelling and adhesive agent, and as a stabilizer working to enhance the functionality of a material [158], just as we attempt to use it in this thesis (**chapter 3**).

2.3.5. PolyP-releasing hydrogels

PolyP-carrying materials have received increased attention due to the physiologically beneficial properties of polyP. Very few polyP-containing hydrogels have been developed, however. Recently, a polyhedral oligomeric silsesquioxane (POSS)-cored polyphosphate and polysaccharide-based injectable hydrogel was developed for cartilage regeneration [159]. Other hydrogels have used polyphosphates in polysaccharide-based hydrogels wastewater treatment

[160], and tissue engineering purposes [161]. The common theme between these hydrogels is the use of polyphosphate as a structural component of the hydrogel; in this regard, very few polyP-releasing hydrogels have been developed. Furthermore, even fewer polyP hydrogels have been developed for fracture healing applications [162]; the majority of these have consisted of polyP-containing nanoparticles and ceramics [27, 163, 164]. In this study, we attempt to formulate a hydrogel that releases polyP for enhanced fracture healing.

Chapter 3: Novel thermoresponsive and injectable inorganic polyphosphate-releasing hydrogel for fracture healing applications

Authors: Rayan Ben Letaifa[1,2,3], Deepak S. Chauhan[4], Chang-sheng Wang[4], Hu Zhang[4], Paul A. Martineau[1,2,3], Xavier Banquy[4], Rahul Gawri[1,2,3]

Affiliations:

1- Division of Orthopaedic Surgery, Department of Surgery, McGill University, Montreal, QC, Canada

2- Regenerative Orthopaedics and Innovation Laboratory, Injury, Repair & Recovery Program, Montreal General Hospital, Research Institute of the McGill University Health Centre, Montreal, QC, Canada

3- Division of Surgical and Interventional Sciences, McGill University, Montreal, QC, Canada

4- Faculty of Pharmacy, Université de Montreal, Montreal, QC, Canada

Keywords: Inorganic polyphosphates, poloxamers, drug delivery, sustained release, fracture repair, mast cells, bone tissue engineering

Abstract

Bone fractures account for a significant proportion of musculoskeletal injuries. Fractures associated with underlying disorders are particularly detrimental to the individual and to health care authorities. Consequently, novel therapeutic approaches for bone tissue regeneration are required to help circumvent fracture complications. Therapeutic approaches utilizing bioactive compounds that modulate the body's response to injury represent new and exciting alternatives

that target early fracture events to promote bone repair. This work presents the development of a novel thermoresponsive composite hydrogel combining poloxamer and Gellan gum with optimal sol-to-gel transition at physiological temperatures. This hydrogel is augmented with inorganic polyphosphates (polyP) and shows controlled release over a period coinciding with the inflammatory phase of fracture healing. Biocompatibility studies show no cytotoxic effects and cell adherence comparable to standard tissue culture plastic. Furthermore, given its proposed role in early fracture immunomodulation, we investigated the chemotactic effect of polyP on mast cell and macrophage analogs through AI-powered single-cell tracking. We showed for the first time, to the best of our knowledge, that polyP could direct mast cell chemotaxis in a concentration-dependent manner, but not macrophages, further suggesting polyP could play a key role in coordinating initial inflammatory events at the fracture site. Taken together, our novel hydrogel could serve as a bioactive drug delivery device purposed for assisted bone tissue regeneration.

1. Introduction

Bone fractures are amongst the most commonly occurring musculoskeletal injuries. Fracture repair is usually successful; however, approximately 5-10% of fracture patients will experience complications such as malunions, delayed unions, or non-unions [49, 106]. Fractures of long bones such as the tibia or the femur are particularly difficult to manage, and the risk of complications contributes significantly to reduced quality of life and post-trauma disability [107]. Fractures endured in high-energy trauma and associated with significant soft tissue damage, such as open fractures, are particularly susceptible to non-union [5, 6]. Patients with chronic diseases also have an increased baseline risk for non-union [165] .

The treatment for non-healing bone injuries can be challenging and requires a comprehensive approach. Many non-unions will require corrective revision surgeries, and these can sometimes be unsuccessful [2, 111, 112]. Surgical treatment of these complications typically includes implantation of autologous or non-autologous bone grafts, debridement, electrical stimulation, or biological enhancement therapy such as percutaneous injection of bone marrow [113], or bone morphogenic protein (BMP) [115, 166]. These however bring along a set of distinct issues including high cost of treatment, unintended bone growth, inflammatory complications, and infection [117, 118]. As such, innovative therapeutic approaches are required to circumvent fracture complications and promote bone repair.

Inorganic polyphosphates (polyP) are linear chains of orthophosphate residues linked by high-energy phosphoanhydride bonds. PolyP is ubiquitous in nature [17, 26], and modulates important physiological processes in a highly dose and chain-length dependent manner [36, 167]. PolyP can drive the osteogenic differentiation of mesenchymal stem cells (MSCs) by upregulating the expression of several osteogenic transcription factors including Runx2 and Sox9 [33, 164]. Moreover, polyP initiates the Fibroblast growth factor 23 (FGF23) signalling pathway to induce proliferation and osteogenic differentiation of MSCs via upregulation of osteopontin (OPN), osteocalcin (OC), and Osteoprotegerin (OPG) expression [34]. Additionally, polyP plays a substantial role in both inflammatory and coagulation processes. PolyP is released from degranulating platelets at the site of injury [22], and is a potent modulator of blood coagulation and fibrinolysis [11]. Furthermore, it functions as a driver of inflammation by participating in contact pathway-driven bradykinin generation through proteolysis of high molecular weight kininogen [168]. It has also been suggested that polyP may exert a proinflammatory effect by activating NF-κB [169], and by interacting with chemokines to modulate inflammatory reactions

[170]. In mast cells and basophils, polyP co-localizes with serotonin in secretory granules, indicating a potential role in the regulation of mast cell inflammatory function [13].

Mast cells are tissue-resident immune cells and are unique due to their large electron-dense secretory granules [171]. These secretory granules contain a broad range of pre-formed mediators required for optimal fracture healing, including biologically active amines, heparin, pro-inflammatory cytokines, and growth factors [92]. During initial events at the fracture site, mast cells play a critical role in regulating fracture-induced inflammation, mainly by releasing IL-6, and influencing innate immune cell recruitment [97, 172]. Previously, we have shown in a murine model of unicortical window defect of mast cell-deficient $Kit^{W\text{-}sh/W\text{-}sh}$ mice that healing was delayed due to compromised replacement of woven bone with compact bone and associated impaired re-vascularization [9]. Additionally, in a c-kit independent $Cpa3^{Cre/+}$ model, bone healing was also impaired as demonstrated by decreased cortical bridging, bone mineralization, and vascularization [10]. Another group showed that in the absence of mast cells, levels of pro-inflammatory cytokines IL-6, IL-1β, and chemokine CXCL1 were significantly reduced and that the recruitment of neutrophils and macrophages to the fracture site was also impaired [98]. Taken together with their ability to ability to respond to specific stimuli [99, 100], their significant involvement in early fracture healing highlights mast cells as potential targets for immunotherapy in assisted bone repair.

Hydrogels are increasingly being investigated as local drug delivery vehicles owing to their adaptable characteristics, controllable degradation, and capacity to protect labile pharmaceuticals [120, 121]. Poloxamers, also referred to as Pluronics, are non-ionic surfactants and tri-block co-polymers that have undergone extensive research and application within the pharmaceutical and biomedical domains. These applications include a wide range of functions, notably drug delivery

systems [147]. Poloxamers are amphiphilic molecules comprised of hydrophilic poly(ethylene oxide) (PEO) blocks and hydrophobic poly(propylene oxide) (PPO) blocks and are able to form micelles in an aqueous environment at a critical micelle concentration (CMC) [148]. Combined with their ability to undergo sol-to-gel transition at physiological temperatures [149], poloxamers show potential for effective administration of polyP in the context of bone tissue regeneration.

Considering the ability of polyP to promote MSC osteogenic differentiation and modulate pro-inflammatory responses in key players of the initial fracture healing process, such as mast cells, our objective is to use the intrinsic bioactivity of this molecule to augment bone repair by localized delivery and maintenance of optimal concentration of polyP at the fracture site. In this study, we investigated the immuno-tactic effects of polyP on key fracture healing immune cells, mast cells and macrophages, and developed a novel thermoresponsive and injectable composite hydrogel purposed as a polyP delivery vehicle for fracture healing applications.

2. Materials and Methods

2.1. Materials

The materials and chemicals were commercially procured as follows: Pluronic® F108 (PEO_{133}-PPO_{50}-PEO_{133}, Mn = 14,600 Da) [Cat no. 583062, BASF Industrial Formulators North America, Florham Park, New Jersey, USA], Gellan Gum [Cat. No. J63423.30, ThermoFisher Scientific, Saint Laurent, Quebec, Canada], polyP-45 solutions [average 45 phosphate residues, Cat No. S4379, Sigma-Aldrich, Oakville, Ontario, Canada] were prepared by dissolving sodium phosphate glass in distilled water, 3-mercaptopropionic acid (MPA) [Cat No. M5801, Sigma-Aldrich, Oakville, Ontario, Canada], N-vinyl caprolactam (NVCL) [Cat No. 415464, Sigma-Aldrich, Oakville, Ontario, Canada], Azobisisobutyronitrile (AIBN) [Cat No. 441090, Sigma-

Aldrich, Oakville, Ontario, Canada], and Chitosan (low molecular weight) [Cat No. 448869, Sigma-Aldrich, Oakville, Ontario, Canada].

2.2. Cell Culture

Mouse osteoblastic cell line MC3T3-E1 cell line [Cat No. CRL-2595, Cedarlane Corporation, Burlington, Ontario, Canada] was cultured in Minimum Essential Medium-α (MEM-α) [Gibco™, Cat. No. 12571063, Fisher Scientific, Ottawa, Ontario, Canada] supplemented with 10% fetal bovine serum (FBS) [Gibco Cat. No. 12483020, Life Technologies, Burlington, Ontario, Canada] and 1% antibiotic-antimycotic (anti/anti) [Cat No. 15240062, Fisher Scientific, Ottawa, Ontario, Canada]. Mouse monocyte/macrophage cell line J774A.1–TIB-67 and human bone marrow mesenchymal stem cells (hBMMSC) [RoosterBio® Catalog No. RoosterVial™-hBM, Frederick, Maryland, USA] were cultured in Dulbecco's Modified Eagle's Media (DMEM) [Gibco™, Cat. No 11965092, Fisher Scientific, Ottawa, Ontario, Canada] and supplemented with 10% FBS [Gibco™ Cat. No. 12483020, Life Technologies, Burlington, Ontario, Canada], 2 mM GlutaMAX™ [Gibco™ Cat. No. 35050061, Fisher Scientific, Ottawa, Ontario, Canada] and 1% anti/anti [Gibco™ Cat No. 15240062, Fisher Scientific, Ottawa, Ontario, Canada]. Rat basophilic leukemia cell line RBL-2H3 [Cat. No. CRL-2256, Cedarlane Corporation, Burlington, Ontario, Canada] was maintained in RPMI-1640 (R8758) [Gibco™, Cat. No. A1049101, Fisher Scientific, Ottawa] supplemented with 10% FBS [Gibco™, Cat. No. 12483020, Fisher Scientific, Ottawa, Ontario, Canada] and 1% anti-anti [Cat No. 15240062, Fisher Scientific, Ottawa, Ontario, Canada]. All cell cultures were maintained in standard cells with 5% CO_2 at 37 °C in 98% relative humidity.

2.3. Chemotactic Analysis

PolyP-directed chemotaxis of cell lines RBL-2H3 and J774A.1-TIB-67 were studied using Ibidi® μ-Slide chemotaxis microfluidic chips [Cat. No. 80326, Ibidi® USA Inc., Fitchburg, Wisconsin, USA]. Cells were allowed to grow to confluency, trypsinized and 6 μL of cells at a density of $3.0x10^6$ cells per ml were subsequently seeded into the cell compartment of the chemotaxis chip. Seeded chambers were then incubated for three hours for cell attachment to take place. Sterile gauze wetted with sterile was placed inside a tissue culture plate alongside the chip in order to maintain humidity and minimize the evaporation of media (**Figure 1A**). Following proper cell attachment, media reservoirs were filled, and a series of polyP-45 concentrations were added to the chemoattractant well as per the supplier's protocols. The central migration chamber was visualized at 10X magnification and the μ-Slide chemotaxis chips were then imaged over a period of 24 hours using a Zeiss Laser Scanning Confocal LSM780 microscope. Conditions during imaging were maintained at 37°C and 5% CO_2. Images at a magnification of 10X were captured every five minutes and were collated to produce a time-lapse video of five frames per second. Videos produced were imported into the FastTrackAI™ software [MetaViLabs, Austin, Texas, USA] and the chemotaxis was analyzed. The minimum threshold of cell movement was set at 2 μm, and the cell movement was analyzed based on a cumulative assessment of time segments.

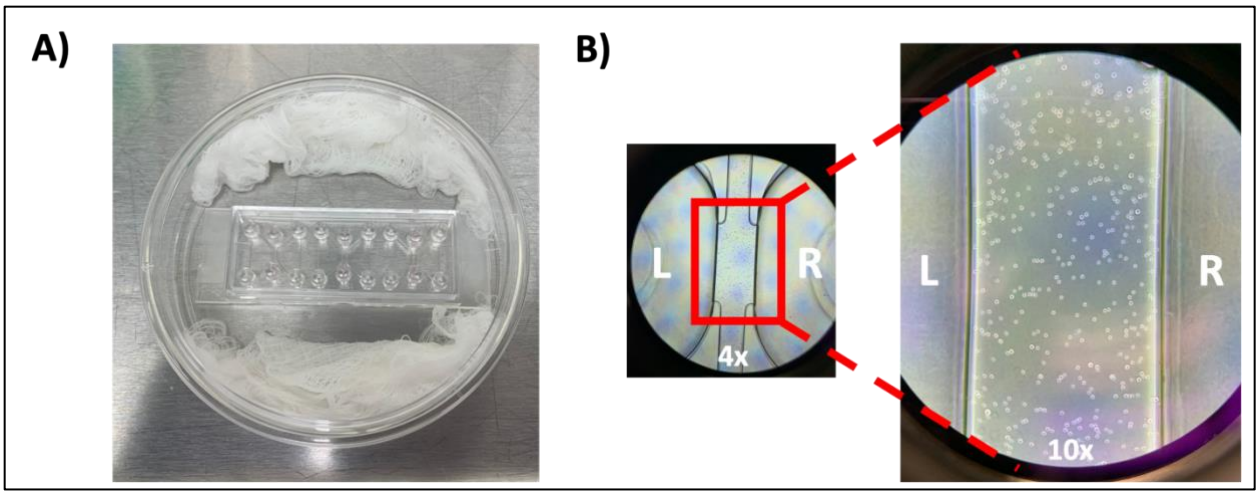

Figure 1: (A) Schematic of μ-Slide chamber will cells seeded in each middle compartment. Sterile gauze was wetted with sterile PBS before incubation. (**B)** Experimental setup for polyP-guided chemotaxis of immune cells. The microfluidic μ-Slide chemotaxis chip consists of a chemoattractant-filled compartment on the left **(L)**, and a plain media-filled compartment on the right **(R)**. The central chamber (**red box**) is used for seeding cells and is the region of interest for live cell imaging. The inset shows RBL-2H3 mast cell analog cells seeded for chemotaxis studies.

2.3. Chitosan-g-PNVCL Synthesis

PNVCL-COOH was first synthesized and subsequently grafted onto Chitosan using a modified procedure from Prabaharan *et al*. [173] and Indulekha *et al*. [174]. NVCL (37.35 mmol), MPA (3.278 mmol) and AIBN (0.304 mmol) were dissolved in 25 mL of isopropanol. The reaction mixture was bubbled with argon for 30 minutes to remove oxygen. The flask was put in a preheated 80°C oil bath for 8 hours. Following the reaction, the product was precipitated with excess diethyl ether and subsequently dried under vacuum. Thereafter, the product was re-dissolved in 25 mL of deionized water and was dialyzed in cellulose membrane tubing (molecular weight cut-off 2 kDa) against distilled water for 3 days. Finally, the solution was lyophilized to obtain the solid PNVCL-COOH. Chitosan (0.5 g) was dissolved in 100 mL of 1% acetic acid under uniform stirring. The

solution of PNVCL–COOH (0.5 g in 5 mL deionized water) was also prepared and then added to the Chitosan solution. A solution of 1-Ethyl-3-(3-dimethylaminopropyl) carbodiimide (0.096 g) and N-Hydroxysuccinimide (0.0575 g) in 5 mL of deionized water was subsequently added into the reactant mixture dropwise. The reaction was allowed to continue for 8 hours at room temperature under constant stirring. Finally, the reaction mixture was purified by dialysis against distilled water for 3 days using cellulose membrane tubing (molecular weight cut-off 12 kDa). The final product was obtained by freeze-drying.

2.4. Sol-gel Transition Testing and Hydrogel Preparation

Hydrogel formulations and sol-gel transition times were tested using poloxamers PF-31, PF-88, PF-108, and PF-237, Gellan gum, and poly-N-vinyl caprolactone (PNVCL). Varying concentrations of each chemical component were tested in different combinations using the tube inversion method in a 37°C bead water bath. Formulations resulting in the fastest sol-to-gel transition were chosen to be doped with polyP-45. The formulation chosen to be tested via release assay was prepared by dissolving PF-108 in distilled water or polyP-45 solution for 24 hours. Gellan gum was subsequently added and allowed to be dissolved for an additional 24 hours. For polyP-doped hydrogels, polyP-45 solutions (0.0, 1.0, 2.5, 5.0, and 10.0 mM) were used in place of distilled water.

2.5. Release Assay

Hydrogel formulations (with and without polyP-45 doping) were encapsulated inside cellulose-based dialysis bags with a molecular weight cut-off (MWCO) of 6-8 kDa. These were subsequently placed inside a screw-top plastic container filled with 50 mL of pre-warmed phosphate-buffered saline (PBS, Ca^{2+}/Mg^{2+} free, pH 7.2) at 37°C. Each container was incubated

and placed on a shaker at 37°C. 5 mL samples were collected from each container at time points 0, 2, 4, 6, 12, 24, 48, 72, 96, and 120 hours; at each time a 5 mL sample was collected, 5 mL of fresh PBS was replenished in each compartment. All samples were stored at 4°C immediately after collection until further processing and analysis. The experiments were repeated three times.

2.6. Quantification of polyP

Stock solutions of polyP-45 were prepared and used to generate a standard curve as previously described [39]. 100 μL of each collected sample and polyP stock solution was combined with 50 μL of 10 μg/ml DAPI in 10 mM Tris-HCL buffer on Corning® solid black flat transparent bottom 96-well plates [Cat. No. 3904, Corning®, St. Louis, Missouri, USA]. Fluorescence measurements were taken on a Tecan Infinite™ 200 Microplate Reader at excitation and emission wavelengths 358 nm and 407 nm, respectively. The fluorescence read data were transferred to MS Office Excel™ and graphs were plotted to trace the concentration of polyP-45 in the solution at each time point.

2.7. Rheological Assessments of Hydrogel Compositions

Prepared hydrogel formulations of increasing polyP-doping (0 mM polyP-45, 1 mM polyP-45, 5 mM polyP) were inserted into a rough surface Couette flow geometry (cup and bob diameters of 18.066 mm and 16.66 mm, respectively). Rheological assessments were undertaken using a stress-controlled Physica MCR 501 rheometer (Anton Paar, Graz, Austria). All samples were subjected to a shear rate of 1000 s^{-1} for 60 seconds to remove the history effect by breaking down any previously existing networks. A dynamic temperature sweep was performed at 1 rad/s in the identified viscoelastic regime at a heating rate of 0.5°C/minute in the temperature range between 25-40°C. Additionally, a strain sweep was conducted from 0.1%-1000% with a frequency of 1

rad/s at a temperature of 37°C to characterize the loss of hydrogel network structure. The storage modulus (*G'*), loss modulus (*G''*), and related complex viscosity ($|\eta^*|$) were recorded as functions of temperature and time every 30 seconds. Samples were covered with a thin layer of low-viscosity mineral oil to prevent water evaporation.

2.8. Scanning Electron Microscopy

Hydrogel formulations doped with the following concentrations 0.0, 1.0, 2.5, 5.0, and 10.0 mM of polyP-45 were incubated at 37°C for 10 minutes before immediately placing in a -80°C for 2 hours. All hydrogel samples were subsequently freeze-dried for 3 days in preparation for scanning electron microscopy (SEM). Samples were cleaned using nitrogen gas, and images were obtained using a Phenom^{TM} XL Desktop SEM [ThermoFisher Scientific, Saint Laurent, Quebec, Canada] at magnifications 1000x, 2500x, 5000x, 10000x, and 15000x with an acceleration voltage of 15 kV.

2.9. Cell Adhesion Assay

Approximately 100 μL of each hydrogel sample was placed into the wells of a 48-well tissue culture-treated plate to fully cover the bottom of each well. Plates were incubated at 37°C for 10 minutes before cell seeding. MC3T3-E1, RBL-2H3, J774A.1, and hBMMSC cells were seeded at a density of 25,000 cells/well in a total volume of 500 μL per well. Cells were incubated for 24 hours. The media was then collected, the hydrogel was washed with PBS, and the liquid was once again collected. Cells found in the collected liquid were subsequently counted with a Neuber's hemacytometer. All cell adhesion experiments were repeated three times with biological triplicates.

2.10. Cell Viability Assay

Cell viability was studied by staining cells seeded on the polyP-45 releasing hydrogels with Live/Dead^{TM} [Cat. No. R37601, Sigma-Aldrich, Oakville, Ontario, Canada]. Approximately 100 μL of the hydrogel formulation was inserted into a 48-well tissue culture-treated plate to fully cover the bottom of each well. Plates were incubated at 37°C for 10 minutes prior to cell seeding. In separate experiments, MC3T3-E1, RBL-2H3, J774A.1, and hBMMSC cells at a density of 25,000 cells/well in a total volume of 500 μL per well. Cells were incubated for 24 hours. The media was subsequently removed and washed twice with Ca^{2+}/Mg^{2+} free PBS. Live/Dead^{TM} was then added to each well and incubated for 10 minutes prior to imaging using fluorescence microscopy [EVOS M5000, ThermoFisher Scientific, Saint Laurent, Quebec, Canada].

2.11. Ex-vivo Adhesion Testing

Rabbit legs were obtained from a local abattoir and all the soft tissue surrounding the femur and tibia were dissected. A 5 mM polyP-45-loaded hydrogel was mixed with 3% (v/v) toluidine blue (0.1% in 70% ethanol) to facilitate visualization. The hydrogel was injected onto the bone, and inversion trials were undertaken immediately to assess adherence to the bone. Following inversion trials, the bone with the hydrogel adhered to it was incubated at 37°C for two hours. Further inversion trials were undertaken after incubation to assess adherence at physiological temperatures.

2.12. Statistical Analysis

All analyses were performed with GraphPad Prism 9.0; one-way or two-way ANOVA with Tukey multiple comparison tests were used. All results are expressed as the means ± SEM.

Significance was set at $p \leq 0.05$. All experimental procedures were repeated three times with biological triplicates.

3.4. Results

3.1. In-vitro polyP-mediated chemotaxis

To characterize the chemotactic effects of polyP on mast cell and macrophage chemotaxis, we used analogs of both cell types, RBL-2H3 and J774A.1-TIB-67, respectively. **Figure 2A** shows the migration plots of RBL-2H3 cells within the region of interest. Here the chemoattractant gradient was established on the x-axis, with migration in the direction of the negative x-axis indicating movement towards the gradient, and migration in the direction of the positive x-axis direction indicating movement away from the chemoattractant gradient. Similarly, **Figure 2B** shows the migration plots of cell line J774A.1-TIB-67 within the region of interest with the same chemoattractant gradient configuration. The migration plots of both cell lines show the trajectories over six hours of live cell imaging within the μ-Slide chemotaxis chamber.

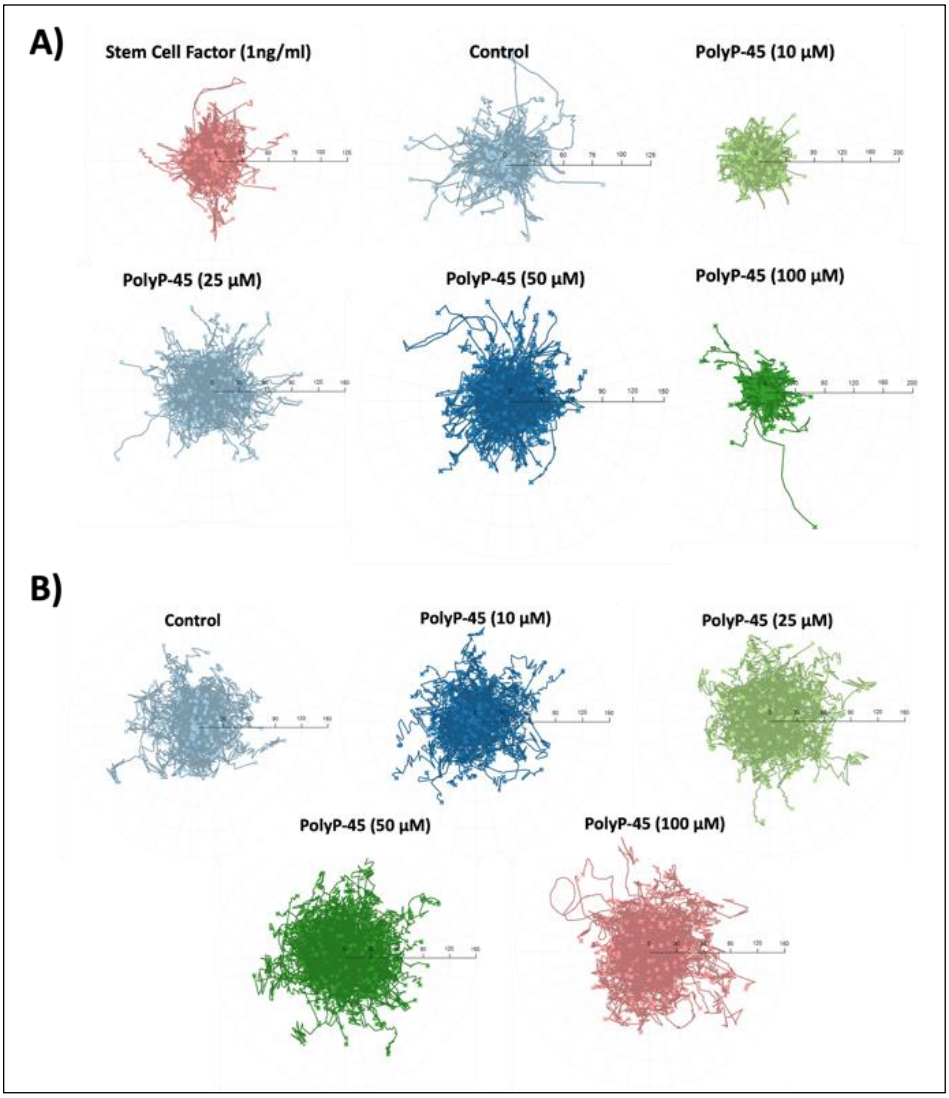

Figure 2: Cellular trajectories in the presence of different polyP-45 concentrations. **(A)** shows migratory plots of mast cell analogue cell line RBL-2H3. **(B)** shows migratory plots of macrophage analogue cell line J774A.1-TIB-67. Control conditions consisted of two chambers filled with plain media without the addition of any chemoattractant. Movement to the left of the origin indicates movement towards the chemoattractant gradient.

Cell trajectories in **Figure 2** were quantified based on center of mass displacement (CoM; measured in µm) in time segments 2, 4, 6, and 8 hours, cumulatively. At time points 2, 4, 6, and 8 hours, an applied stem cell factor gradient produced a significant directional RBL-2H3 center of

mass displacement when compared to a plain media null control. RBL-2H3 cells showed a dose-responsive chemotactic effect towards polyP-45 (**Figure 3A**). The stem cell factor-dependent chemotaxis was highly non-uniform as indicated by the Rayleigh test value ($p < 0.0001$). A chemoattractant gradient produced by a polyP concentration of 50 μM also resulted in a directional RBL-2H3 center of mass displacement towards the polyP gradient compared to the plain media null control; this chemoattractant-driven movement was also non-uniform as confirmed by the Rayleigh test ($p < 0.0001$). By contrast, polyP concentrations of 10, 25, and 100 μM did not produce a significant center of mass displacement when compared to the plain media control, and their movement was also non-uniform. (Rayleigh test: $p < 0.0001$). The J774A.1-TIB-67 cell migration is presented in **Figure 3B**. PolyP-45 gradients with concentrations 10, 50, and 100 μM did not produce significant center of mass displacement when compared to the plain media control; polyP concentrations of 50 and 100 μM produced uniform movement ($p > 0.05$) while 10 μM produced non-uniform movement ($p < 0.05$) as indicated by their respective Rayleigh test values. Conversely, a polyP concentration of 25 μM produced an anti-directional center of mass displacement when compared to the plain media control, and its movement was non-uniform ($p < 0.05$).

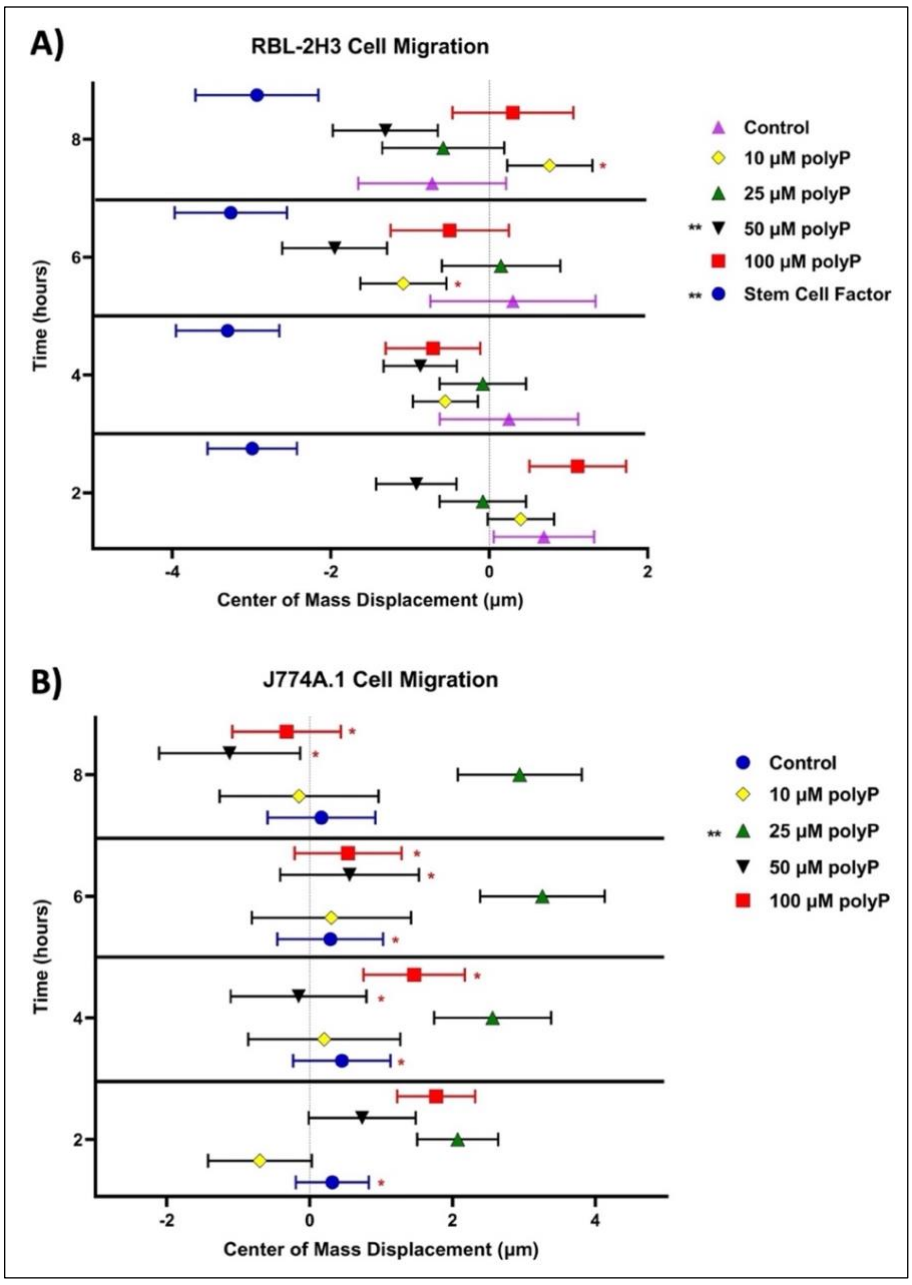

Figure 3: (A) shows murine mast cell analogue RBL-2H3 displacement in response to a polyP-45 chemotactic gradient. **(B)** shows murine macrophage analogue cell line J774A.1-TIB-67 displacement in response to a polyP-45 chemotactic gradient. Negative displacement indicates movement towards a chemotactic gradient. **(**)** indicates a movement that is significant ($p < 0.05$) with respect to cell movement in the control group over all time points. **(*)** indicates uniform movement (Rayleigh test $p > 0.05$). Rayleigh test values are statistical values dependent on the

uniformity of movement. 'p' values < 0.05 suggest non-uniform movement, thus indicating directed chemotactic movement. Data presented as mean ± SEM.

The speed (μm/min) of moving cells in response to varying concentrations of polyP-45 is presented in **Figure 4**. When RBL-2H3 cells were subjected to a polyP gradient (**Figure 4A**), the speed of their movement was significantly increased when compared to the plain media control. The maximum cell movement speed was noted when cells were subjected to a 25 μM polyP-45 concentration. Stem cell factor did not significantly increase average cell movement speed in comparison to the control plain media. Conversely, the presence of polyP-45 at concentrations of 10 and 25 μM decreased J774A.1-TIB-67 cell movement speed significantly **(figure 4B)** compared to the control plain media; however, when subjected to a polyP-45 concentration of 100 μM, the average speed of cell movement was increased. A polyP concentration of 100 μM did not significantly alter the cell movement speed.

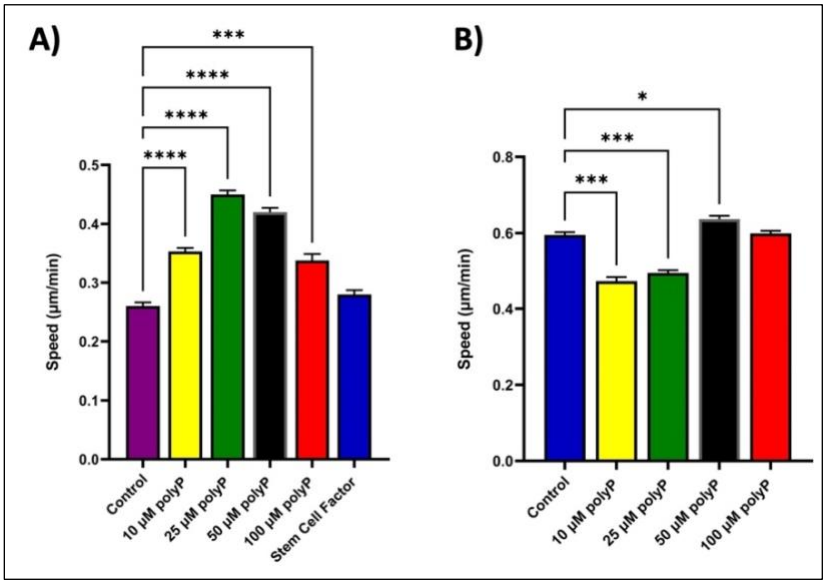

Figure 4: (A) shows RBL-2H3 and **(B)** shows J774A.1-TIB-67 cell movement speed (μm/min) in response to different chemoattractants. Data presented as mean ± SEM. (*: $p < 0.05$, **: $p < 0.01$, ***: $p < 0.001$, ****: $p < 0.0001$)

3.2. Hydrogel fabrication

In order to develop a hydrogel delivery system for the controlled localized delivery of polyP, we selected polymer candidates chitosan-g-PNVCL, poloxamers P-F31, P-F88, P-F108, and Gellan gum due to their reported characteristic biocompatibility and thermoresponsive behaviour. Accordingly, we tested several combinations of these polymers using the tube inversion method (**Table 1**). Chitosan-g-PNVCL hydrogels up to 5% w/v did not undergo sol-to-gel transition. Conversely, chitosan-g-PNVCL combined with Gellan gum underwent a sol-to-gel transition in more than five minutes when combined with low concentrations of Gellan gum, and immediately formed a hydrogel when combined with high concentrations of Gellan gum. All poloxamers at a concentration of 20% w/v underwent sol-to-gel transition: P-F31 and P-F237 did so in more than five minutes of incubation while P-F88 did so in approximately two minutes and 45 seconds, and P-F88 in approximately 30 to 45 seconds. Given their relatively short sol-to-gel transition times, P-F88 and P-F108 were selected to be combined with firstly chitosan-g-PNVCL and secondly with Gellan gum. The combination of P-F88 (20% w/v) with chitosan-g-PNVCL (1.5% w/v) resulted in a slightly shortened sol-to-gel transition time than P-F88 alone, while no changes in sol-to-gel transition were observed when P-F108 (20% w/v) was combined with chitosan-g-PNVCL (1.5% w/v). Thereon, we combined P-F108 (20% w/v), due to its rapid sol-to-gel transition, with Gellan gum at concentrations 1%, 2%, and 3% w/v. The combination with Gellan gum at a concentration of 1% w/v did not significantly change the transition time, while the combination with Gellan gum at concentrations of 2% and 3% w/v yielded a near-immediate

sol-to-gel transition. The finalized hydrogel formulation consisting of 20% (w/v) PF-108 and 3% (w/v) was chosen as the lead drug delivery candidate for further experiments.

Table 1		
Chitosan-g-PNVCL + Gellan Gum combination Composition % (weight/volume)	**Gel Formation at 37°C**	**Sol-to-gel transition time**
Chitosan-g-PNVCL (1.5%)	No	N/A
Chitosan-g-PNVCL (3%)	No	N/A
Chitosan-g-PNVCL (5%)	No	N/A
Chitosan-g-PNVCL (0.75%) + Gellan Gum (0.75%)	Yes	> 5 min.
Chitosan-g-PNVCL (1.5%) + Gellan Gum (1.5%)	Yes	> 5 min.
Chitosan-g-PNVCL (3%) + Gellan Gum (3%)	N/A	0 s
Chitosan-g-PNVCL (5%) + Gellan Gum (5%)	N/A	0 s
Poloxamers - 20% (w/v)	**Gel Formation at 37°C**	**Sol-to-gel transition time**
P-F31	Yes	> 5 min.
P-F88	Yes	2 min 45 s
P-F108	Yes	30 - 45 s
P-F237	Yes	> 5 min.
Poloxamers + Chitosan-g-PNVCL % (w/v)	**Gel Formation at 37°C**	**Sol-to-gel transition time**
P-F88 (20%) + Chitosan-g-PNVCL (1.5%)	Yes	2 min. 30 s
P-F108 (20%) + Chitosan-g-PNVCL (1.5%)	Yes	30 - 45 s
Poloxamers + Gellan Gum % (w/v)	**Gel Formation at 37°C**	**Sol-to-gel transition time**
P-F108 (20%) + Gellan Gum (1%)	Yes	30 – 45 s
P-F108 (20%) + Gellan Gum (2%)	N/A	0 s
P-F108 (20%) + Gellan Gum (3%)	N/A	0 s

Table 1: Gelation trials were done at 37ºC through the tube inversion method. Several compounds were used including Chitosan-g-PNVCL, poloxamers (P-F31, P-F88, P-F108, P-F237), and Gellan gum. Compositions where gel formation at 37ºC is indicated as **N/A** were hydrogels prior to

immersion in a 37ºC water bath. Compositions where sol-to-gel transition is indicated as **N/A** never underwent sol-to-gel transition.

3.3. PolyP release

Previously, we showed polyP with a chain length of 45 phosphate units (polyP-45) to have the greatest anabolic effect on chondrocytes [36]. To simulate the release of polyP-45 and characterize its release profile from the hydrogel, we employed an open-compartment model drug diffusion test over 120 hours (five days) with hydrogels containing five different concentrations of polyP-45. The hydrogels consisting of 20% (w/v) PF-108 and 3% (w/v) supplemented with 1.0 mM and 10.0 mM polyP exhibited a peak in cumulatively available polyP after 48 hours. In contrast, the hydrogels containing 2.5 mM and 5.0 mM polyP showed a peak in cumulatively available polyP after 24 hours **(figure 5A)**. The polyP concentration within the diffusion compartment exhibited a rapid increase during the initial 24-hour period, which was subsequently sustained for a duration of 120 hours. The achievement of maximum concentration occurred at the 24-hour mark of the diffusion process, except in the case of the hydrogel doped with 1.0 mM polyP. The maximum concentration of polyP in the diffusion compartment demonstrated a direct correlation with the concentration of polyP present in the hydrogel **(Figure 5B)**.

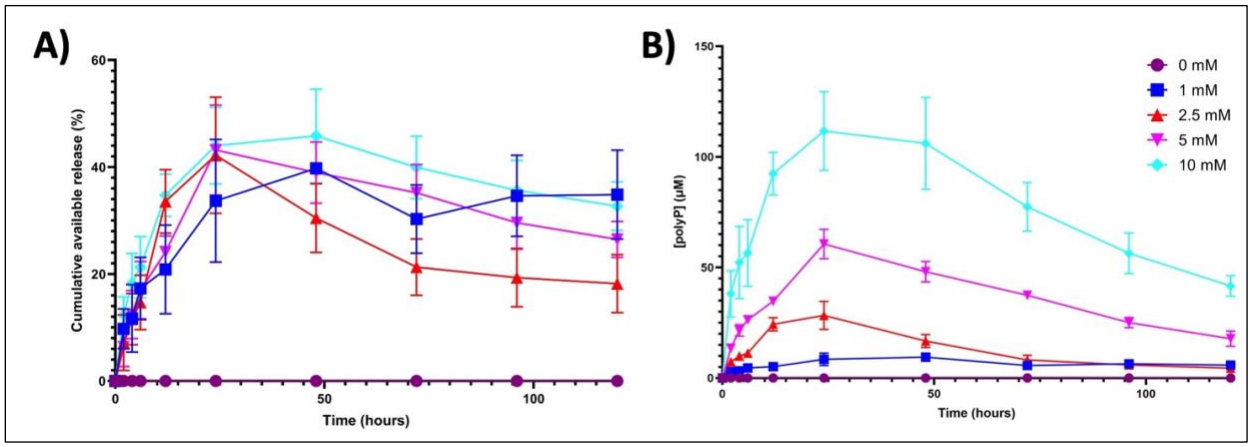

Figure 5: Panel **(A)** shows polyP-45 concentration in the supernatant in an open-compartment model. PolyP concentration external to the hydrogel increases rapidly over the first 24 hours and is sustained throughout the evaluated period of five days, with a peak concentration shown at 24 hours. Panel (**B**) shows the cumulatively available released polyP over five days. Data presented as mean ± SEM.

3.4. Hydrogel Characterizations

To characterize the viscoelastic properties of the hydrogel, a temperature and strain sweep were undertaken with increasing concentrations of polyP-45 in the hydrogel. The findings of the temperature sweep (1 Hz; 25-40 ºC) are shown in **Figure 6A**. All hydrogels exhibited an increase in their viscoelastic moduli as temperature increased, indicating an enhancement of mechanical properties. The observed increase can be divided into three distinct regions: (1) an initial phase with a moderate and stable increase in both storage (*G'*) and loss (*G"*) moduli, (2) a subsequent phase characterized by a significant and rapid increase in both moduli and (3) a final phase characterized by resolution in the increasing slope of the viscoelastic moduli. The storage modulus values of all hydrogels were significantly higher than loss modulus values, indicating the presence of an elastic and consolidated hydrogel structure. The hydrogels comprising polyP displayed higher *G'* and *G"* values compared to the hydrogel without polyP supplementation. The hydrogel doped with 1.0 mM polyP exhibited greater values of *G'* and *G"* compared to the hydrogel containing 5.0 mM polyP within the final phase.

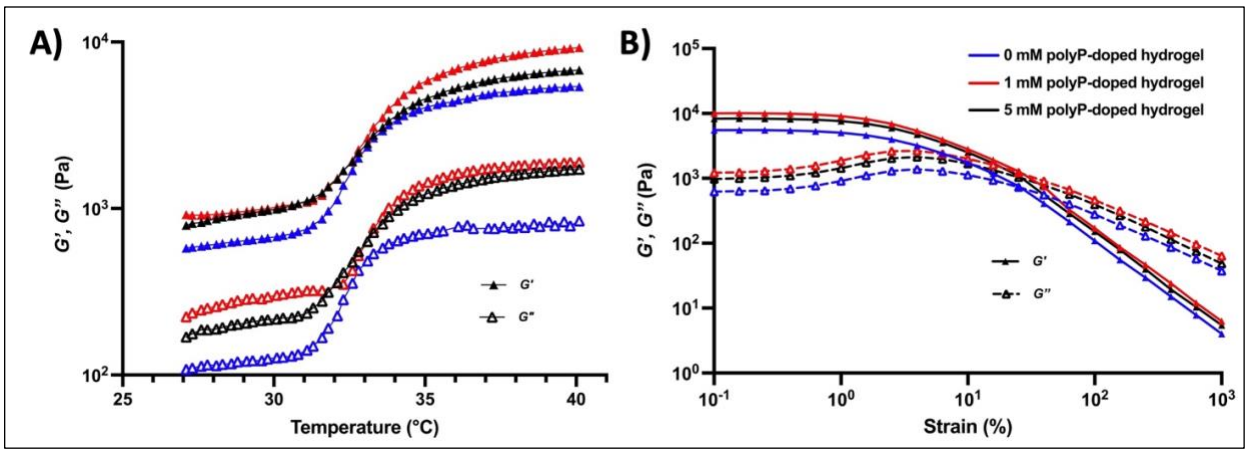

Figure 6: (**A**) Temperature sweep of polyP-loaded hydrogels shows doping-dependent elastic properties with increasing temperature. (**B**) Strain sweep shows *G'* decreasing and *G"* modulus increasing and intersecting at approximately 40% strain. The intersection of both moduli with respect to strain is independent of polyP-doping.

The strain sweep rheological response of the hydrogels is presented in **Figure 6B**. The hydrogels exhibited a viscoelastic region spanning from 0.1% to approximately 10% for all three hydrogels whereby all *G'* values were larger than *G"* values. The point at which the hydrogel structure began to break down was seen at an estimated critical shear strain of 20%. The point of intersection between *G'* and *G"* was seen at around 40% strain inside the within the non-linear viscoelastic region, indicating a transition from mostly elastic behaviour to predominantly viscous behaviour.

Freeze-dried hydrogels containing increasing polyP concentrations were imaged by scanning electron microscopy (**Figure 7**). All hydrogels exhibited similar network structures with micro- and nanopores when observed at 5000x magnification. However, observation at higher magnification revealed morphological differences between the different hydrogels. Hydrogels with lower concentrations of polyP showed considerably larger pores, while hydrogels with higher concentrations of polyP revealed smaller pores with a sponge-like network structure.

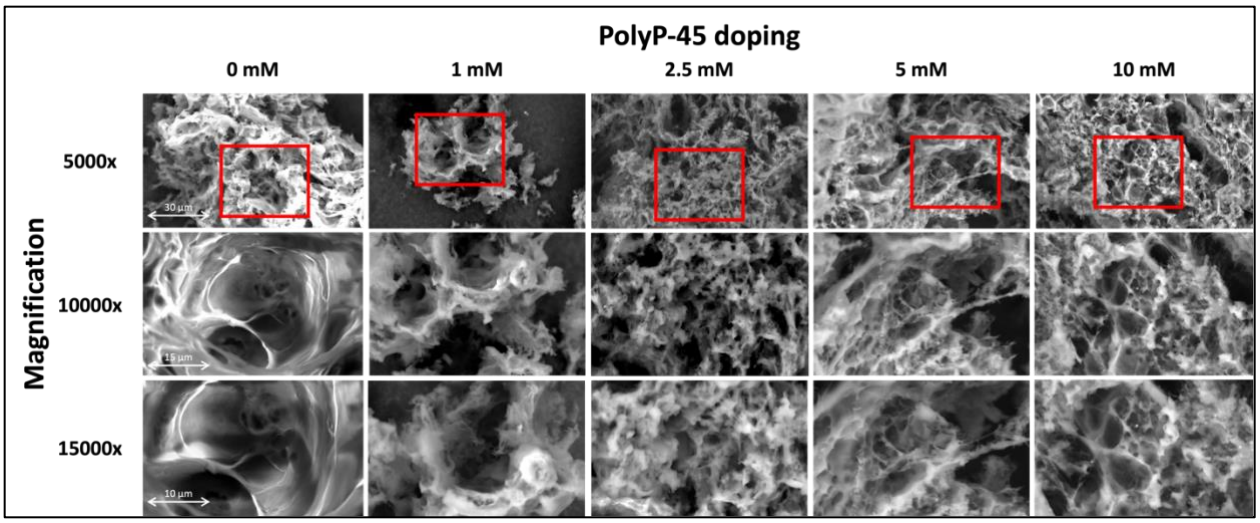

Figure 7: Scanning electron microscopy (SEM) of freeze-dried hydrogel formulations with varying polyP-45 doping to observe hydrogel porosity and cross-linking network. Red boxes indicate the region of interest on which the magnification was focused.

3.5. Cell viability and adhesion

To assess cell viability and monitor cytotoxicity of the polyP-45 supplemented hydrogel, four cell types representing the cells at the fracture site were tested, including MC3T3-E1 (murine osteoblasts), RBL-2H3 (murine mast cell analogue), J774A.1-TIB-67 (murine macrophage analogue), and hBMMSC (human bone marrow-derived mesenchymal stromal cells), a Live/Dead^{TM} assay was employed as shown in **Figure 8 (A, B, C, D)**. The data analyses revealed no cytotoxic effects of the hydrogel after 24 hours in culture, and the number of dead cells was negligible for all cell types. In addition, the images show the cells adhered to the surface of the hydrogel with uniform distribution. The capacity for these cells to adhere to the hydrogel containing increasing polyP concentrations was quantified and compared to adherence on standard tissue culture plastic (STP) **Figure 8 (E, F, G, H)**. For all cell types, no significant differences could be observed between hydrogels containing polyP and STP 24 hours post-seeding ($p > 0.05$).

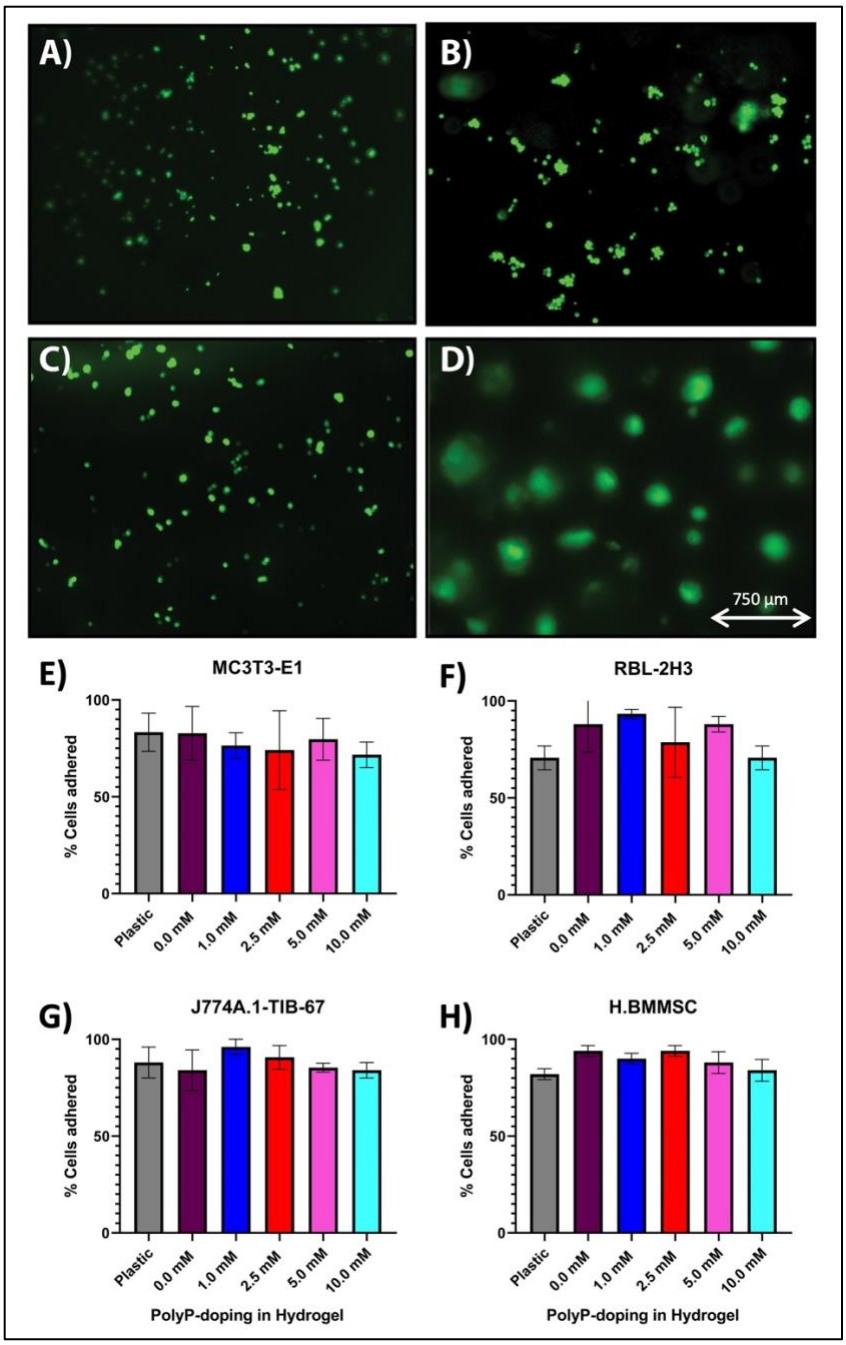

Figure 8. Cell viability study using LIVE/DEAD with cells (**A**) MC3T3-E1, (**B**) RBL-2H3, (**C**) J774A-TIB-67, and (**D**) hBMMSCs cultured on the hydrogel. Live and dead cells were stained green and red, respectively. No cytotoxic effects could be observed after 24 hours of culturing. Panels **E, F, G, and H** show quantification of cell adhesion to the hydrogel supplemented with varying concentrations of polyP-45, 24 hours post-incubation. Cell adhesion to the hydrogel was

not significantly different from cell adhesion on standard tissue culture plastic ($p > 0.05$; all panels). Data presented as means ± SEM.

3.6. Ex-vivo adhesion testing

Rabbit legs were dissected, and the femurs and tibias were excised for ex-vivo hydrogel adhesion testing. The polyP-doped hydrogel containing 5 mM of polyP-45 was administered through injection onto the bones exhibited strong adhesion to the bony surface, and retained its structural integrity, even under rigorous inversion (**Figure 9A**). Additionally, there were no changes to the structural integrity of the hydrogel on the bone after incubation at 37 ºC for two hours (data not shown). The polyP-doped hydrogel was also injected onto the articular surface of the femoral condyles, and the hydrogel adhered to the cartilage surface and retained its structural integrity when subjected to rigorous inversion (**Figure 9B, 9C).** Similarly, no changes in structural integrity could be observed when incubated at 37 ºC for two hours (data not shown).

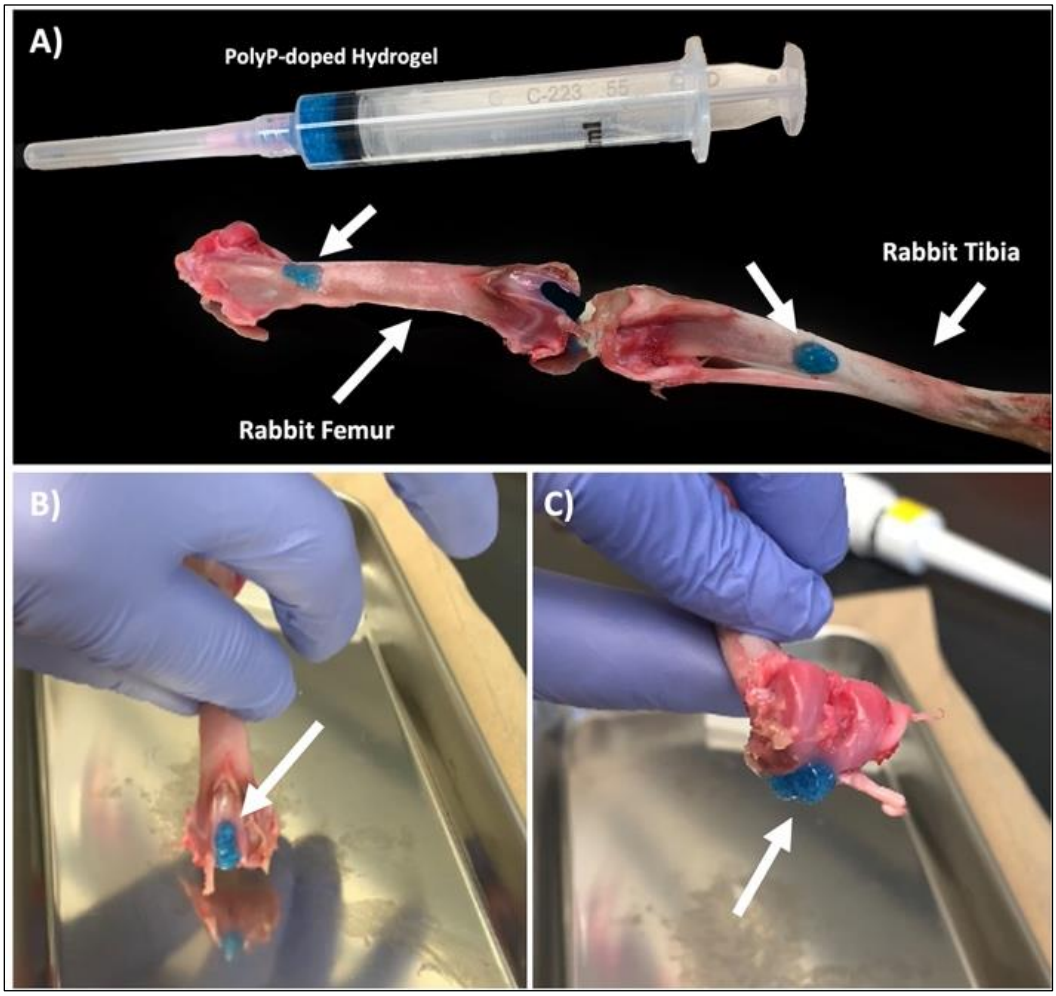

Figure 9. Ex-vivo hydrogel adhesion to the bone. Rabbit femur and tibia were used. The hydrogel supplemented with 5 mM polyP-45 was doped with toluidine blue for visualization. The hydrogel was able to adhere to the bone after injection, and its structure was retained after rigorous inverting **(A)**. Additionally, the hydrogel was injected onto the articular surfaces of the femoral condyles, where it was able to retain its shape (**B**) and remained intact after inversion (**C**). No changes in structural integrity could be observed when incubated at physiological temperatures for up to two hours.

4. Discussion

To our knowledge, this is the first study of its kind to investigate the role of polyP as a chemoattractant and immunomodulator of immune cell migration, with an overarching aim of developing a controlled-release polyP delivery system to be implanted at the fracture site. The ultimate goal of this hydrogel will be to optimally attract immune cells and thereon prevent the occurrence of fracture complications. PolyPs are released in substantial quantities at the fracture site, and thus maintaining the optimal concentration and chain length at the fracture site may be a viable strategy for tissue engineering of bone tissue in a fracture setting. This biodegradable hydrogel could also subsequently act as a scaffold for bone-forming cells to migrate and deposit bone minerals.

Bone fractures acute traumatic events that can have adverse hemodynamic effects depending on the location, traumatic force, and the type of fracture incurred [175]. The initial cellular processes at the fracture site aim at arresting bleeding to preserve the hemodynamic equilibrium, and thereon the body's fracture repair machinery in an orchestrated sequence of cellular and molecular events, initiates the process of fracture healing [64]. Platelets during clot formation become "activated" and release their intracellular cargo comprised of growth factors, cytokines, and chemokines via degranulation [176]. Degranulating platelets also release polyP in substantial quantities [11, 168], which play a major role in the process of coagulation [28, 177]. Recent studies have also demonstrated the strong immunomodulatory roles of polyP [178, 179]. PolyP plays a role in the pro-inflammatory actions of mast cells with polyP of chain lengths similar to those released by platelets were found to co-localize with serotonin, but not with histamine, indicating a potential role in the regulation of mast cell inflammatory function [13]. We used a microfluidic chemotaxis chip and analyzed the data with AI-powered analytical software to

conduct qualitative and quantitative assessments of the dose-dependent chemoattractive effects of polyP. The murine mast cell analogue RBL-2H3 cells showed a dose dependant center of mass (CoM) displacement with the maximal cellular movement at 50 µM concentration of polyP-45 **(Figure 2A & 3A)**, though the response did not surpass the magnitude of stem cell factor (SCF) induced chemoattraction. The cells also showed non-uniform movement, indicating that the chemotactic effect for each cell was in part independent of the individual cells under observation. Some studies suggest that SCF induces mast cell chemotaxis via PLCγ-mediated production of DAG and IP3 [180], whereas other studies report that mast cell chemotaxis is mediated by transient receptor potential melastatin 4 channel (TRPM4) calcium channels [181], with both the mechanisms releasing intracellular Ca^{2+} followed by actin rearrangements and chemotactic response. This could be a possible mechanism for the polyP-induced mast cell chemotaxis as our team has previously shown that polyP causes Ca^{2+} fluxes and increased intracellular concentrations [36]. The speed of the cell migration was maximal at 25 µM and 50 µM **(Figure 4A)**, thus indicating that the local charge densities of polyP-45 and its interaction with divalent cations in the media solution may play a role as polyP is internalized with Ca^{2+} when polyP-induced Ca^{2+} fluxes occur [36]. This however needs to be further investigated. Human macrophage analogue cell line J774A.1-TIB-67 on the other hand did not show an effective chemotactic response to treatment with polyP in the timeframe of investigation, but showed delayed movement between 6-8 hours timepoint at 100 µM concentration and movement away from the polyP loaded chambers at 25µM concentration **(Figure 2B & 3B)**. The speed of cell migration was also very slow and comparable to controls in the cumulative experimental observation timeline **(Figure 4B)**. This could be due to different mechanisms of action of polyP in macrophages or different macrophage

surface receptor morphology, altering the co-translocation of polyP and Ca^{2+}, or alternatively due to the electrostatic repulsion and limited space for movement.

With the demonstration that polyP could direct immune cell chemotaxis, we sought to develop a hydrogel polyP delivery system that could release polyP at the fracture site to attract immune cells. Given that polyP has a dose-dependent effect, regulated and sustained polyP release is necessary to counteract *in-situ* metabolism and elimination to achieve the desired therapeutic effect. Therefore, we tested polymer candidates that had the potential to encapsulate highly charged anionic molecules. Thermoresponsive hydrogels are useful due to their temperature-controlled physical properties, drug release, and minimally invasive applications [134]. Here we showed that a composite poloxamer PF-108 hydrogel had the best potential for thermoresponsive behaviour and injectability when combined with 1.5% chitosan-g-PNVCL (w/v) or 3% Gellan Gum (w/v) (**Table 1**). Gellan gum is a water-soluble complex polysaccharide and commonly used in the food industry, and more recently for tissue engineering purposes [151, 155, 158, 182]. Due to the highly liquid texture of P-F108, we exploited the thickening properties of Gellan gum [156], in combination with P-F108, to provide structural integrity and malleability, while retaining its injectable properties.

Figure 5 illustrates that the release of polyP is dependent upon the initial doping of polyP in the hydrogel formulation. For all tested polyP-containing hydrogel formulations, the cumulatively available polyP ranged from approximately 35-50% after 48 hours, and approximately 20-40% after 120 hours (**Figure 5A**). This reveals that a significant proportion of encapsulated polyP remains within the hydrogel formulation. Considering the poly-anionic structure of polyP, it is not surprising that polyP may have strong interactions with hydroxyl groups in the PEO groups of P-F108 and Gellan gum. The decreasing polyP content after 48 hours is

attributed to the decreasing polyP concentration within the testing compartment and may partially be due to its interaction with degrading hydrogel components, mainly PEO chains of P-F108. The *in vitro* degradation may also be masking the true cumulative release of polyP, and thus polyP content could be higher at later time points in the study. Further studies are required to determine the reason for diminishing polyP concentration. This release study showed that the concentration of polyP outside of the hydrogel could be tuned by altering the initial concentration of polyP within the hydrogel **(Figure 5B)**. The observed sustained release of polyP from the hydrogel ensures that polyP is available at the site of implantation and coincides with the inflammatory phase of fracture healing (up to day 5), where immune cell mediators, including mast cells, play a critical role in establishing the inflammatory micro-environment required for optimal fracture healing [79-83, 183].

The thermoresponsive behaviour of this hydrogel, attributed to P-F108, is well demonstrated in **Figure 6**. Although the formulation is initially a hydrogel as characterized by its initial larger *G'* than *G"* value, as temperature increases, both values increase in magnitude, indicating strengthening in the structural network through micellization [148]. The thickening properties of Gellan gum likely led to the hydrogel formation at room temperature, while the increasing *G'* value is due to the thermoresponsive properties of poloxamers. The increase in structural integrity at physiological temperatures could provide additional retention of polyP for longer-term release and ensure stability *in vivo*. SEM images of the freeze-dried hydrogel formulation reveal a sponge-like porous structure (**Figure 7**). Given that poloxamers form micelles with hydrophobic PPO cores, it is plausible that polyP may navigate through a matrix comprised of hydrophilic PEO chains and Gellan gum and therefore released from the hydrogel by diffusion.

Poloxamers and Gellan gum are biocompatible materials and are well-established in the pharmaceutical and food industries, respectively [149, 151, 184, 185]. Here we tested the biocompatibility of the composite formulation with murine and human cell lines (**Figure 8A-H)** The cell type chosen was based on the cells generally involved in the early events of fracture healing. All four chosen types of cells tested showed a high percentage of live cells after 24 hours of culture on the surface of the hydrogel. This demonstrates the cytocompatibility of the polyP-releasing hydrogel formulation; the non-exothermic nature of the hydrogel formation reaction also facilitates this. This further establishes poloxamer-based hydrogels as a drug delivery and tissue engineering tool.

In developing this polyP-releasing hydrogel, we envisioned it to be malleable, injectable, and able to undergo sol-to-gel transition at physiological temperatures. With these properties in mind, the hydrogel could be injected into the fracture gap with or without internal fixation and would be retained at the fracture site after muscle and skin wound closure. To test whether this gel would adhere to bony tissue, we tested its adherence on rabbit femur and tibias by recreating a window defect fracture model *ex vivo*. The adhesion studies showed the hydrogel adhering to the uninjured cortical bone tissue following plastering, and to the edges of the cortical bone window defect when administered via injection **(Figure 9 A-C)**. Furthermore, upon testing, the hydrogel also adhered to the cartilage surface of the knee joint, due to the highly adhesive properties associated with Gellan gum [182]. This finding demonstrates the applications of this hydrogel could be extended to the treatment of arthritis by acting as an injectable drug delivery vehicle.

This novel polyP-releasing hydrogel could improve fracture healing in two ways: 1) by enhancing the recruitment and maturation of circulating mast cells at the fracture site [10, 98, 103, 186] during early fracture healing, leading to the release of growth factors and cytokines that attract

other immune cells such as macrophages and neutrophils, and 2) by enhancing the osteogenic differentiation of migrating bone marrow mesenchymal stem cells to bridge the fracture gap [12, 27, 34]. Mast cells are critical regulators of early inflammatory events in fracture healing and contain a wide range of pro-osteogenic growth factors and cytokines [96]. They secrete a plethora of mediators that enhance angiogenesis via different pathways, particularly through direct secretion of VEGF, SCF, TGFβ, PDGF, EGF, TNFα and bFGF, among others [103, 104]. The optimal and regulated homing of the immune cells at the fracture site will enhance the migration of bone-forming cells and the differentiation of mesenchymal stem cells to form the fracture callus [186-188]. Nevertheless, a sustained presence of immune cells can lead to delayed or defective healing and an overactive mast cell reaction could result in such an outcome [189, 190]. The proposed function of polyP delivery at the fracture site is to enhance the early recruitment of mast cells, and thereby increase the concentration of pro-osteogenic mediators at the fracture site, to accelerate and enhance healing, and avoid potential complications. This hydrogel was optimized to release polyP within five days, coinciding with the inflammatory phase of the fracture healing [64], after which polyP release is exhausted and cleared by tissue non-specific alkaline phosphatases (TNAP) from circulation.

There are however a few limitations to this study. Platelets are known to release a wide range of polyP chain lengths; as such, additional chain lengths must be evaluated within our hydrogel system and chemotaxis studies. Furthermore, the efficacy of the hydrogel at releasing polyP and enhancing fracture repair *in vivo* still needs to be investigated. We aim to test this as a follow-up to this study in a murine femoral unicortical window defect model previously developed and validated by our group [9, 10, 191-193]. In addition, the exact mechanism of action of polyP in immune cell recruitment still needs to be elucidated.

5. Conclusion

In conclusion, we have developed a novel immunomodulatory polyP-releasing thermoresponsive poloxamer-based hydrogel system for enhanced fracture applications. The hydrogel is tunable, and the amount of polyP doped can be adjusted without significant changes to the hydrogel properties. This delivery strategy will optimally enhance the recruitment of immune cells during the initial phases of fracture healing to enhance fracture healing and circumvent the complications of fracture healing such as non-unions and malunions. This could have a significant impact on the quality of life of fracture-bearing patients and reduce the burden on the healthcare system.

Acknowledgements: The study was made possible through operating grants from The Montreal General Hospital Foundation (CODE LIFE), le Réseau de thérapie cellulaire tissulaire et génique du Québec (ThéCell Network), le Réseau de recherche en santé buccodentaire et osseuse (RSBO) and Natural Sciences and Engineering Research Council of Canada (NSERC) Discovery Grants awarded to Rahul Gawri. Rayan Ben Letaifa was supported by the Canadian Institutes of Health Research (CIHR) Canada Graduate Scholarship-Masters (CGS-M) and a graduate research fellowship from the Research Institute of McGill University Health Center (RI-MUHC). We would also like to thank the staff at the Molecular Imaging Core of the Research Institute of McGill University Health Center (RI-MUHC) for helping us set up the chemotaxis experiments.

Author contributions: RBL conducted the experiments, analyzed the data, and wrote the manuscript. **DSC** helped with the characterization of the hydrogel using scanning electron microscopy. **CW** helped perform rheological analyses of the hydrogels. **HZ** synthesized chitosan-

g-PNVCL and provided expertise in material preparation for scanning electron microscopy. **PAM** analyzed the data, provided expertise, and provided help with the unicortical defect model. **XB** provided lab space and materials, designed experiments, analyzed data, and wrote the manuscript. **RG** conceived the study, designed the experiments, secured funding, provided lab space and materials, oversaw experimental procedures, and wrote the manuscript. All authors have approved the draft of the manuscript.

Chapter 4: Discussion

Practical therapeutic approaches for bone tissue regeneration are a rapidly emerging topic in the field of orthopaedic research. The development of novel drug delivery devices that bolster the body's capacity for regeneration, as an alternative to the currently inefficient standard of practice, are crucially important given the high clinical relevance of non-healing fractures [194, 195]. Bone repair comprises a highly ordered sequence of events and depends heavily on the interactions between the skeletal system and the immune system, particularly during early stages of healing. Despite the ongoing improvements made in therapeutic approaches to non-healing fractures, complications remain particularly common in patients with inflammatory disorders [165]. In this study, we conceived a novel drug delivery system optimized for in-vivo implantation and sustained polyP release at the fracture site. Furthermore, we showed for the first time, to the best of our knowledge, that polyP could direct mast cell analog chemotaxis.

Previously, the finding of polyP in platelet-dense granules led to the discovery of its role in pro-inflammatory, hemostatic, and fibrinolytic actions [177]. PolyP of chain lengths similar to those released by platelets were found to co-localize with serotonin, but not with histamine, indicating polyP may play a role in the pro-inflammatory actions of mast cells [13, 196]. With the use of microfluidic chemotaxis chips and AI-powered single-cell tracking, we showed that polyP-45 could direct mast cell chemotaxis in a concentration-dependent manner. For our studies, we used mast cell analog RBL-2H3, a widely used mast cell model [197], for its ease of culture and use in our chemotaxis devices. A polyP concentration of 50 μM had the greatest CoM displacement when compared to other polyP concentrations, and the only statistically significant CoM movement when compared to other polyP concentrations (**Figure 3A**). This effect was especially pertinent after six hours of incubation within the chemotaxis chamber, where a 50 μM polyP

concentration was not significant to the movement observed when treated with stem cell factor (SCF), a known mast cell chemoattractant [198, 199]. Although the mechanism of polyP inflammatory modulation is poorly understood, the mechanism by which polyP interacts with mast cells could be attributed to G-protein coupled $P2Y_1$ purinergic receptors found on the surface of mast cells [200]. These receptors function by inducing calcium transients that activate further downstream signal transduction mechanisms. The link between polyP and $P2Y_1$ receptors, as well as several findings of polyP action related to calcium signalling [201, 202], further suggest a potential interaction between polyP and mast cell $P2Y_1$ receptors through the calcium signalling [181]. Alternatively, given the potent ability of mast cells to respond to damage-associated molecular patterns (DAMPs) [6, 100, 203], polyP could act as a DAMP and thus trigger a mast cell response. Taken as a whole, this finding provides a proof-of-concept basis that polyP can act as a chemoattractant for mast cells. Macrophage analogs J774A.1-TIB-67, on the other hand, did not demonstrate a chemotactic response towards polyP gradients (**Figure 3B**). Macrophages, in response to polyP treatment, displayed mainly uniform movement, indicating a lack of directional movement. Interestingly, a poly concentration of 25 μM directed macrophage movement away from the polyP gradient with non-uniform motion, indicating a directional displacement. Although $P2Y_1$ receptor-encoding mRNA could be detected in human monocytes [204, 205], as well as in M1-like pro-inflammatory macrophages, there is limited evidence of functional $P2Y_1$ receptor expression in monocyte or monocyte-derived cells [206]. This could explain the lack of response to polyP treatment; however, further investigations into the mechanism of action of polyP are required.

The treatment of polyP had a gradually increasing effect on the mast cell average speed of movement (**Figure 4A**). All tested polyP concentrations had a statistically significant increase in average speed when compared to plain media control. Although stem cell factor had the greatest impact on directional cell movement, its treatment did not have a significant effect on the average speed of cell movement. Macrophages showed a different trend where lower concentrations of polyP slowed the average speed (10 μM, 25 μM) whereas higher concentrations increased the average speed (50 μM) (**Figure 4B**). Cell surface electrostatic repulsion could contribute to the increases in average cell speed observed with mast cells. A similar phenomenon was previously observed in the context of myelin membrane adhesion [207] and in T cell receptor signalling [208]. This however does not explain the slowing of macrophage average speed. The baseline average speed of moving macrophages is higher than that of mast cells (**Figure 4**), and higher than the increased speed of mast cells after polyP treatment. The high baseline speed of movement of macrophages could therefore be slowed as a consequence of electrostatic repulsion and a limited space for movement, as seen with polyP treatment at concentrations 10 μM, and 25 μM (**Figure 4B**). The increased speed of movement seen with a treatment of 50 μM polyP could be due to the overcoming of a concentration threshold, where the increased negative charge density results in a slightly increased macrophage average speed of movement. This however does not explain the unaffected speed of cell movement when treated with 100 μM polyP.

Figure 5 demonstrates that the release of polyP is dependent upon the initial doping of polyP in the hydrogel formulation. For all tested polyP-containing hydrogels, the cumulatively available polyP ranged from approximately 35-50% after 48 hours, and approximately 20-40% after 120 hours (**Figure 5A**). This reveals that a significant proportion of encapsulated polyP remains within the hydrogel formulation. Considering the poly-anionic structure of polyP, it is not

surprising that polyP may have strong interactions with hydroxyl groups in the PEO groups of P-F108 and Gellan gum. The decreasing polyP content after 48 hours is attributed to the decreasing polyP concentration within the compartment and may partially be due to its interaction with degrading hydrogel components, mainly PEO chains of P-F108. The in-vitro degradation may also be masking the true cumulative release of polyP, and thus polyP content could be higher at later time points in the study. Further studies are required to determine the reason for diminishing polyP concentration. This release study showed that the concentration of polyP outside of the hydrogel could be tuned by altering the initial concentration of polyP within the hydrogel (**Figure 5B**). The observed sustained release of polyP from the hydrogel ensures that polyP is available at the site of implantation, and coincides with the inflammatory phase of fracture healing, where immune cell mediators, including mast cells, play a critical role in establishing the inflammatory micro-environment required for proper healing [97, 98, 187]. Therefore, attracting mast cells during this period is paramount to have the desired mast cell-derived therapeutic effect.

The thermoresponsive behaviour of this hydrogel, attributed to P-F108 [209], is well demonstrated in **Figure 6**. Although the formulation is initially a hydrogel, as characterized by its initial larger *G'* than *G"* value, as temperature increases, both values increase in magnitude, indicating strengthening in the structural network through micellization [148]. The thickening properties of Gellan gum likely led to the hydrogel formation at room temperature, while the increasing *G'* value is due to the thermoresponsive properties of poloxamers. The increase in structural integrity at physiological temperatures could provide additional retention of polyP for longer-term release and ensure stability *in vivo*. SEM images of the freeze-dried hydrogel formulation reveal a sponge-like porous structure (**Figure 7**). Although the desiccated form of the hydrogel does not reveal an accurate depiction of the structure of the hydrogel [210, 211], it

provides insights into how the polyP is encapsulated into the hydrogel and subsequently released. Given that poloxamers form micelles with hydrophobic PPO cores, it is plausible that polyP may navigate through a matrix comprised of hydrophilic PEO chains and Gellan gum and therefore released by diffusion.

In this study, we showed the biocompatibility of our composite formulation in **Figure 8A, B, C, and D**. All four types of cells tested were alive after 24 hours of culture on the surface of the hydrogel. No cytotoxic effects could be observed. The lack of dead cells in this Live/Dead™ staining could be attributed to the washing of dead cells in preparation for imaging. Further studies are required to assess long-term viability and to assess the potential for cell proliferation on the surface of the hydrogel. Cell adhesion to the hydrogel was not significantly different from plasma-treated tissue culture plastic (**Figure 8E, F, G, H**). Some variation in adhesion was observed with RBL-2H3 cells with hydrogels with different polyP-doping (**Figure 8E**) but remained consistent for other cell types. Ex-vivo adhesion studies revealed the hydrogel adhered to bony tissue after injection or plastering of the hydrogel. Furthermore, the hydrogel adhered to the cartilage surface of the knee joint, demonstrating its highly adhesive properties linked to Gellan gum [158]. Additionally, the hydrogel could be plastered into a unicortical femoral defect window and formed a uniform surface with neighbouring cortical bone (data not shown). This adhesive property is necessary for the polyP to be delivered at the site of implantation and to maximize local therapeutic action.

This novel polyP-releasing hydrogel could improve fracture healing in 2 ways: 1) by enhancing the recruitment of mast cells to the fracture site [97, 103] during early fracture healing and 2) by enhancing the osteogenic differentiation of mesenchymal stem cells [27, 34]. As previously stated, mast cells are critical regulators of early inflammatory events in fracture healing

[98] and contain a wide range of pro-osteogenic growth factors and cytokines [103]. Mast cells secrete many mediators that enhance angiogenesis through different pathways, particularly through direct secretion of VEGF, SCF, TGFβ, PDGF, EGF, TNFα and bFGF, among others [96, 103, 171, 212]. Furthermore, they influence angiogenic processes through the recruitment of macrophages and other immune cells [187, 188], and secrete a variety of proteases that degrade connective tissue matrix to provide the means for new vessel formation, and thereby promote tissue regeneration [186]. Accordingly, stimulation of neo-vascularization through localized mast cell-based immunotherapy could be used to treat or prevent non-healing fractures, including non-unions and delayed unions. Nevertheless, the sustained presence of immune cells can lead to delayed or defective healing and an overactive mast cell reaction could result in such an outcome [190, 213]. The proposed function of polyP delivery is to enhance the early recruitment of mast cells, and thereby the concentration of pro-osteogenic mediators at the fracture site, to accelerate and improve healing, and circumventing potential complications. As previously stated, this hydrogel was optimized for polyP release within five days, coinciding with the inflammatory phase of fracture healing [214]. Therefore, an overactive mast cell reaction is not suspected after this period as demonstrated by our polyP release profile study (**figure 5**). The application of this hydrogel will be tested in an *in-vivo* murine model of unicortical femoral defect previously developed by our group [9, 10, 191-193]

As previously mentioned, injectable hydrogels are attractive choices because of their capacity to administer therapeutic agents like drugs or bioactive compounds aimed at tissue regeneration. In this context, these injectable hydrogels offer a minimally invasive alternative to implant surgery by effectively filling irregularly shaped bone or cartilage defect sites. Bone defects and fractures constitute the primary focal points within the realm of bone tissue engineering

inquiries. Defects may arise from various sources such as trauma, infections, tumour resection, or skeletal abnormalities. Notably, the repair of bone defects relies heavily on the extracellular matrix, facilitating signal transduction and material exchange between regenerated tissue and the original bone structure [215]. In mimicking the structure of the extracellular matrix, the composition of hydrogels presents an opportunity to effectively replicate its functionality. As such, hydrogels offer inherent advantages as scaffolds fostering the formation of new bone tissue, exhibiting significant promise in expediting bone synthesis to address these defects [136]. Fractures, conversely, frequently occur due to substantial force or pressure exerted upon the bone. While many fractures can heal without surgical intervention, complex fractures often exhibit poor recovery and frequently necessitate surgical repair [216]. Within contemporary orthopaedic practice, the burgeoning interest in utilizing injectable hydrogels during open reduction and internal fixation procedures for bone healing underscores their burgeoning therapeutic potential. However, the practical application of these hydrogels in such treatments represents a multifaceted approach demanding meticulous preparation and precise execution. The pliable and adherent nature of our hydrogel formulation presents a promising avenue for addressing bone fractures and defects necessitating both surgical and non-surgical interventions. This formulation's adaptability makes it suitable for immediate application following a fracture due to its optimized polyP release profile, strategically designed to coincide with the inflammatory phase of fracture healing, thereby exerting a polyP-mediated immunomodulatory effect. Particularly noteworthy is its potential preventive role in patients with predisposing conditions like diabetes, osteoporosis, and other metabolic diseases, aiming to prevent the occurrence of non-union or malunion. Moreover, in cases where compromised blood supply or impaired angiogenesis is anticipated, such as in diabetic patients [217], the enhanced recruitment of mast cells to the fracture site via polyP release holds

promise for therapeutic benefits. Therefore, this hydrogel could be used pre-emptively with patients with such pre-disposing conditions. However, further in vivo investigations are required to ascertain these potential benefits. For non-displaced fractures, not necessitating surgical intervention, the application of the hydrogel via injection around the fracture site stands as a viable approach. Conversely, in cases requiring open reduction, direct access allows for the application of the hydrogel within the fracture site following internal fixation. In the context of fracture defects, the hydrogel not only functions as an immunomodulator but also serves as a scaffold for facilitating the migration of bone-forming cells, thereby enhancing the efficient bridging of fractured ends. This combined approach of employing the hydrogel in conjunction with fixation devices serves a dual purpose: providing stability to fracture fragments while fostering an environment conducive to bone healing and integration. Despite considerable strides in leveraging hydrogels for bone healing, several challenges persist. The delicate balance between mechanical strength and degradation kinetics, the augmentation of regenerative potential, and the refinement of application methodologies warrant focused attention in further studies. The intricate nature of employing hydrogels to enhance bone healing underscores the importance of considering specific fracture patterns and patient characteristics to delineate the most efficacious clinical implementation techniques.

Platelet-rich plasma (PRP) constitutes a regenerative treatment that has gained immense popularity in a wide array of medical applications including orthopaedic sports medicine, aesthetics and dermatology [218, 219]. PRP is derived from a patient's blood and contains concentrated amounts of platelets, growth factors and other mediators that may promote tissue repair and regeneration [220]. Platelet counts normally range in blood from 150 000/μL to 350 000/μL, whereas PRP injections associated with enhanced healing can contain counts of more than

1 000 000/μL [220]. Its primary goal is to stimulate the body's own healing process, mainly through recruitment, proliferation and differentiation of cells involved in the regenerative process, including immune cells [221]. Interestingly, PRP promotes the expression of osteogenic markers alkaline phosphatase (ALP) and OC [222], as well as chondrogenic markers in MSCs [223, 224]. Although its current regenerative action is attributed to growth factors TGF-β, insulin-like growth factor (IGF), bFGF, VEGF, and platelet-derived growth factor, its specific mechanism of action is yet to be well characterized [27, 225]. Taking into account the very high content of polyP in platelet-dense granules [22, 170] and the similar physiological effects associated with polyP, it is reasonable to suggest polyP may play a significant role in the therapeutic benefits of PRP. As ongoing investigations continue to uncover the potential of polyP, our polyP-releasing hydrogel could potentially serve as a new treatment modality with similar effects to PRP.

Chapter 5: Summary and Conclusion

In conclusion, this composite polyP-releasing biomaterial has the potential to enter the emerging field of bioactive hydrogels for fracture healing applications. As shown, polyP can direct mast cell chemotaxis, which are key players in early fracture healing and could be targeted through polyP delivery to promote healing; however, macrophages did not show directional movement towards polyP. This potentially suggests a new role for polyP in the initial fracture healing cascade. Additionally, not only could polyP provide the metabolic fuel, but polyP released from the hydrogel could enhance the osteogenic differentiation of bone-resident mesenchymal stem cells as previously shown in other studies. Ultimately, this study has validated this novel material for pre-clinical *in-vivo* studies of fracture healing and could aid in improving clinical outcomes and reducing clinical strain.

Bibliography

1. Aldhafian, M., et al., *Patient-dependent factors for fractures union failure among Riyadh population 2016.* Journal of Family Medicine and Primary Care, 2020. **9**(12): p. 6224-6227.
2. Zura, R., et al., *Epidemiology of Fracture Nonunion in 18 Human Bones.* JAMA Surgery, 2016. **151**(11): p. e162775.
3. *Prevalence of metabolic syndrome in the Canadian adult population.* CMAJ, 2019. **191**(5): p. E141.
4. Dziak, R., *Osteoimmunology: cross-talk between bone and immune cells.* Immunol Invest, 2013. **42**(7): p. 657-60.
5. Bahney, C.S., et al., *Cellular biology of fracture healing.* Journal of Orthopaedic Research, 2019. **37**(1): p. 35-50.
6. Muire, P.J., L.H. Mangum, and J.C. Wenke, *Time Course of Immune Response and Immunomodulation During Normal and Delayed Healing of Musculoskeletal Wounds.* Frontiers in Immunology, 2020. **11**: p. 1056.
7. Raghuram, A., et al., *Bone Grafts, Bone Substitutes, and Orthobiologics: Applications in Plastic Surgery.* Semin Plast Surg, 2019. **33**(3): p. 190-199.
8. Taniguchi, H., *Mast cells in fracture healing: an experimental study using rat model.* Nihon Seikeigeka Gakkai Zasshi, 1990. **64**(10): p. 949-957.
9. Behrends, D.A., et al., *Defective bone repair in mast cell deficient mice with c-Kit loss of function.* European Cells & Materials, 2014. **28**: p. 209-221; discussion 221-222.
10. Ramirez-GarciaLuna, J.L., et al., *Defective bone repair in mast cell-deficient Cpa3Cre/+ mice.* PLoS One, 2017. **12**(3): p. e0174396.

11. Morrissey, J.H. and S.A. Smith, *Polyphosphate as modulator of hemostasis, thrombosis, and inflammation.* Journal of Thrombosis and Haemostasis, 2015. **13**(S1): p. S92-S97.

12. Wang, X., H.C. Schröder, U. Schloßmacher, and W.E.G. Müller, *Inorganic Polyphosphates: Biologically Active Biopolymers for Biomedical Applications*, in *Biomedical Inorganic Polymers: Bioactivity and Applications of Natural and Synthetic Polymeric Inorganic Molecules*, W.E.G. Müller, X. Wang, and H.C. Schröder, Editors. 2013, Springer: Berlin, Heidelberg. p. 261-294.

13. Moreno-Sanchez, D., L. Hernandez-Ruiz, F.A. Ruiz, and R. Docampo, *Polyphosphate Is a Novel Pro-inflammatory Regulator of Mast Cells and Is Located in Acidocalcisomes*.* Journal of Biological Chemistry, 2012. **287**(34): p. 28435-28444.

14. Lander, N., C. Cordeiro, G. Huang, and R. Docampo, *Polyphosphate and acidocalcisomes.* Biochem Soc Trans, 2016. **44**(1): p. 1-6.

15. Docampo, R., P. Ulrich, and S.N. Moreno, *Evolution of acidocalcisomes and their role in polyphosphate storage and osmoregulation in eukaryotic microbes.* Philos Trans R Soc Lond B Biol Sci, 2010. **365**(1541): p. 775-84.

16. Azevedo, C. and A. Saiardi, *Functions of inorganic polyphosphates in eukaryotic cells: a coat of many colours.* Biochem Soc Trans, 2014. **42**(1): p. 98-102.

17. Brown, M.R. and A. Kornberg, *Inorganic polyphosphate in the origin and survival of species.* Proc Natl Acad Sci U S A, 2004. **101**(46): p. 16085-7.

18. Rashid, M.H. and A. Kornberg, *Inorganic polyphosphate is needed for swimming, swarming, and twitching motilities of Pseudomonas aeruginosa.* Proc Natl Acad Sci U S A, 2000. **97**(9): p. 4885-90.

19. Rashid, M.H., N.N. Rao, and A. Kornberg, *Inorganic polyphosphate is required for motility of bacterial pathogens.* J Bacteriol, 2000. **182**(1): p. 225-7.

20. Rashid, M.H., et al., *Polyphosphate kinase is essential for biofilm development, quorum sensing, and virulence of Pseudomonas aeruginosa.* Proc Natl Acad Sci U S A, 2000. **97**(17): p. 9636-41.

21. Kuroda, A., et al., *Inorganic polyphosphate stimulates lon-mediated proteolysis of nucleoid proteins in Escherichia coli.* Cell Mol Biol (Noisy-le-grand), 2006. **52**(4): p. 23-9.

22. Ruiz, F.A., C.R. Lea, E. Oldfield, and R. Docampo, *Human platelet dense granules contain polyphosphate and are similar to acidocalcisomes of bacteria and unicellular eukaryotes.* J Biol Chem, 2004. **279**(43): p. 44250-7.

23. Li, C.H., J.M. Bland, and P.J. Bechtel, *Effect of precooking and polyphosphate treatment on the quality of microwave cooked catfish fillets.* Food Sci Nutr, 2017. **5**(3): p. 812-819.

24. Gray, M.J. and U. Jakob, *Oxidative stress protection by polyphosphate--new roles for an old player.* Curr Opin Microbiol, 2015. **24**: p. 1-6.

25. Rao, N.N., M.R. Gomez-Garcia, and A. Kornberg, *Inorganic polyphosphate: essential for growth and survival.* Annu Rev Biochem, 2009. **78**: p. 605-47.

26. Harold, F.M., *Inorganic polyphosphates in biology: structure, metabolism, and function.* Bacteriol Rev, 1966. **30**(4): p. 772-94.

27. Wang, Y., et al., *Progress and Applications of Polyphosphate in Bone and Cartilage Regeneration.* BioMed Research International, 2019. **2019**: p. 5141204.

28. Choi, S.H., S.A. Smith, and J.H. Morrissey, *Polyphosphate accelerates factor V activation by factor XIa.* Thrombosis and Haemostasis, 2015. **113**(3): p. 599-604.

29. Choi, S.H., S.A. Smith, and J.H. Morrissey, *Polyphosphate is a cofactor for the activation of factor XI by thrombin.* Blood, 2011. **118**(26): p. 6963-6970.

30. Nickel, K.F., et al., *The polyphosphate–factor XII pathway drives coagulation in prostate cancer-associated thrombosis.* Blood, 2015. **126**(11): p. 1379-1389.

31. Docampo, R. and S.N.J. Moreno, *Acidocalcisomes.* Cell calcium, 2011. **50**(2): p. 113-119.

32. Kolf, C.M., E. Cho, and R.S. Tuan, *Mesenchymal stromal cells. Biology of adult mesenchymal stem cells: regulation of niche, self-renewal and differentiation.* Arthritis Res Ther, 2007. **9**(1): p. 204.

33. Zhou, G., et al., *Dominance of SOX9 function over RUNX2 during skeletogenesis.* Proc Natl Acad Sci U S A, 2006. **103**(50): p. 19004-9.

34. Kawazoe, Y., et al., *Activation of the FGF signaling pathway and subsequent induction of mesenchymal stem cell differentiation by inorganic polyphosphate.* Int J Biol Sci, 2008. **4**(1): p. 37-47.

35. Wang, X., et al., *The marine sponge-derived inorganic polymers, biosilica and polyphosphate, as morphogenetically active matrices/scaffolds for the differentiation of human multipotent stromal cells: potential application in 3D printing and distraction osteogenesis.* Mar Drugs, 2014. **12**(2): p. 1131-47.

36. Gawri, R., et al., *The anabolic effect of inorganic polyphosphate on chondrocytes is mediated by calcium signalling.* J Orthop Res, 2021.

37. Wiame, J.M., *The Metachromatic Reaction of Hexametaphosphate.* Journal of the American Chemical Society, 1947. **69**(12): p. 3146-3147.

38. Tijssen, J.P., H.W. Beekes, and J. Van Steveninck, *Localization of polyphosphates in Saccharomyces fragilis, as revealed by 4',6-diamidino-2-phenylindole fluorescence.* Biochim Biophys Acta, 1982. **721**(4): p. 394-8.

39. Lee, W.D., et al., *Simple Silica Column–Based Method to Quantify Inorganic Polyphosphates in Cartilage and Other Tissues.* CARTILAGE, 2018. **9**(4): p. 417-427.

40. Streichan, M., J.R. Golecki, and G. Schön, *Polyphosphate-accumulating bacteria from sewage plants with different proceses for biological phosphorus removal.* FEMS Microbiology Ecology, 1990. **6**(2): p. 113-124.

41. Martin, P. and B.A.S. Van Mooy, *Fluorometric Quantification of Polyphosphate in Environmental Plankton Samples: Extraction Protocols, Matrix Effects, and Nucleic Acid Interference.* Applied and Environmental Microbiology, 2013. **79**(1): p. 273-281.

42. Kolozsvari, B., F. Parisi, and A. Saiardi, *Inositol phosphates induce DAPI fluorescence shift.* Biochemical Journal, 2014. **460**(3): p. 377-385.

43. Christ, J.J., S. Willbold, and L.M. Blank, *Polyphosphate Chain Length Determination in the Range of Two to Several Hundred P-Subunits with a New Enzyme Assay and 31P NMR.* Analytical Chemistry, 2019. **91**(12): p. 7654-7661.

44. Christ, J.J., S. Willbold, and L.M. Blank, *Methods for the Analysis of Polyphosphate in the Life Sciences.* Analytical Chemistry, 2020. **92**(6): p. 4167-4176.

45. Müssig-Zufika, M., A. Kornmüller, B. Merkelbach, and M. Jekel, *Isolation and analysis of intact polyphosphate chains from activated sludges associated with biological phosphate removal.* Water Research, 1994. **28**(8): p. 1725-1733.

46. Ohtomo, R., Y. Sekiguchi, T. Kojima, and M. Saito, *Different chain length specificity among three polyphosphate quantification methods.* Analytical Biochemistry, 2008. **383**(2): p. 210-216.

47. Choi, B.K., D.M. Hercules, and M. Houalla, *Characterization of Polyphosphates by Electrospray Mass Spectrometry.* Analytical Chemistry, 2000. **72**(20): p. 5087-5091.

48. Bergh, C., D. Wennergren, M. Moller, and H. Brisby, *Fracture incidence in adults in relation to age and gender: A study of 27,169 fractures in the Swedish Fracture Register in a well-defined catchment area.* PLoS One, 2020. **15**(12): p. e0244291.

49. Ekegren, C.L., E.R. Edwards, R. de Steiger, and B.J. Gabbe, *Incidence, Costs and Predictors of Non-Union, Delayed Union and Mal-Union Following Long Bone Fracture.* International Journal of Environmental Research and Public Health, 2018. **15**(12): p. 2845.

50. Sheen, J.R. and V.V. Garla, *Fracture Healing Overview*, in *StatPearls*. 2022, StatPearls Publishing: Treasure Island (FL).

51. Kolar, P., et al., *The early fracture hematoma and its potential role in fracture healing.* Tissue Engineering. Part B, Reviews, 2010. **16**(4): p. 427-434.

52. Ozaki, A., M. Tsunoda, S. Kinoshita, and R. Saura, *Role of fracture hematoma and periosteum during fracture healing in rats: interaction of fracture hematoma and the periosteum in the initial step of the healing process.* Journal of Orthopaedic Science: Official Journal of the Japanese Orthopaedic Association, 2000. **5**(1): p. 64-70.

53. Chung, R., et al., *Roles of neutrophil-mediated inflammatory response in the bony repair of injured growth plate cartilage in young rats.* Journal of Leukocyte Biology, 2006. **80**(6): p. 1272-1280.

54. Bastian, O., et al., *Systemic inflammation and fracture healing.* Journal of Leukocyte Biology, 2011. **89**(5): p. 669-673.

55. Schmidt-Bleek, K., et al., *Initiation and early control of tissue regeneration - bone healing as a model system for tissue regeneration.* Expert Opinion on Biological Therapy, 2014. **14**(2): p. 247-259.

56. Walters, G., I. Pountos, and P.V. Giannoudis, *The cytokines and micro-environment of fracture haematoma: Current evidence.* Journal of Tissue Engineering and Regenerative Medicine, 2018. **12**(3): p. e1662-e1677.

57. Kenkre, J.S. and J.H.D. Bassett, *The bone remodelling cycle.* Annals of Clinical Biochemistry, 2018. **55**(3): p. 308-327.

58. Granero-Moltó, F., et al., *Regenerative Effects of Transplanted Mesenchymal Stem Cells in Fracture Healing.* Stem Cells, 2009. **27**(8): p. 1887-1898.

59. Kitaori, T., et al., *Stromal cell–derived factor 1/CXCR4 signaling is critical for the recruitment of mesenchymal stem cells to the fracture site during skeletal repair in a mouse model.* Arthritis & Rheumatism, 2009. **60**(3): p. 813-823.

60. Gerstenfeld, L.C., et al., *Three-dimensional Reconstruction of Fracture Callus Morphogenesis.* Journal of Histochemistry & Cytochemistry, 2006. **54**(11): p. 1215-1228.

61. Hu, D.P., et al., *Cartilage to bone transformation during fracture healing is coordinated by the invading vasculature and induction of the core pluripotency genes.* Development (Cambridge, England), 2017. **144**(2): p. 221-234.

62. Aghajanian, P. and S. Mohan, *The art of building bone: emerging role of chondrocyte-to-osteoblast transdifferentiation in endochondral ossification.* Bone Research, 2018. **6**: p. 19.

63. Grant, W.T., G.J. Wang, and G. Balian, *Type X collagen synthesis during endochondral ossification in fracture repair.* Journal of Biological Chemistry, 1987. **262**(20): p. 9844-9849.

64. Marsell, R. and T.A. Einhorn, *The biology of fracture healing.* Injury, 2011. **42**(6): p. 551-555.

65. Foster, A.L., et al., *The influence of biomechanical stability on bone healing and fracture-related infection: the legacy of Stephan Perren.* Injury, 2021. **52**(1): p. 43-52.

66. Benulič, Č., et al., *Mechanobiology of indirect bone fracture healing under conditions of relative stability: a narrative review for the practicing clinician.* Acta Bio Medica : Atenei Parmensis, 2021. **92**(Suppl 3): p. e2021582.

67. ElHawary, H., et al., *Bone Healing and Inflammation: Principles of Fracture and Repair.* Seminars in Plastic Surgery, 2021. **35**(3): p. 198-203.

68. Ai-Aql, Z.S., et al., *Molecular mechanisms controlling bone formation during fracture healing and distraction osteogenesis.* Journal of Dental Research, 2008. **87**(2): p. 107-118.

69. Breur, G.J., B.A. VanEnkevort, C.E. Farnum, and N.J. Wilsman, *Linear relationship between the volume of hypertrophic chondrocytes and the rate of longitudinal bone growth in growth plates.* Journal of Orthopaedic Research: Official Publication of the Orthopaedic Research Society, 1991. **9**(3): p. 348-359.

70. Ansari, M., *Bone tissue regeneration: biology, strategies and interface studies.* Progress in Biomaterials, 2019. **8**(4): p. 223-237.

71. Kaderly, R.E., *Primary bone healing.* Semin Vet Med Surg Small Anim, 1991. **6**(1): p. 21-5.

72. Greenbaum, M.A. and I.O. Kanat, *Current concepts in bone healing. Review of the literature.* J Am Podiatr Med Assoc, 1993. **83**(3): p. 123-9.

73. Einhorn, T.A. and L.C. Gerstenfeld, *Fracture healing: mechanisms and interventions.* Nature reviews. Rheumatology, 2015. **11**(1): p. 45-54.

74. Gerstenfeld, L.C., et al., *Fracture healing as a post-natal developmental process: Molecular, spatial, and temporal aspects of its regulation.* Journal of Cellular Biochemistry, 2003. **88**(5): p. 873-884.

75. M, T., K. I, O. K, and G. A, *[Osteoimmunology: new area of research on the associations between the immune and bone systems]*. Polskie Archiwum Medycyny Wewnetrznej, 2001. **105**(5).

76. Ginaldi, L. and M. De Martinis, *Osteoimmunology and Beyond.* Current Medicinal Chemistry, 2016. **23**(33): p. 3754-3774.

77. Baht, G.S., L. Vi, and B.A. Alman, *The Role of the Immune Cells in Fracture Healing.* Current Osteoporosis Reports, 2018. **16**(2): p. 138-145.

78. Butterfield, T.A., T.M. Best, and M.A. Merrick, *The Dual Roles of Neutrophils and Macrophages in Inflammation: A Critical Balance Between Tissue Damage and Repair.* Journal of Athletic Training, 2006. **41**(4): p. 457-465.

79. Kovtun, A., et al., *The crucial role of neutrophil granulocytes in bone fracture healing.* European Cells & Materials, 2016. **32**: p. 152-162.

80. Fan, S., et al., *Macrophages—bone marrow mesenchymal stem cells crosstalk in bone healing.* Frontiers in Cell and Developmental Biology, 2023. **11**.

81. McCauley, J., C. Bitsaktsis, and J. Cottrell, *Macrophage subtype and cytokine expression characterization during the acute inflammatory phase of mouse bone fracture repair.* Journal of Orthopaedic Research, 2020. **38**(8): p. 1693-1702.

82. Chen, L., et al., *Changes in macrophage and inflammatory cytokine expressions during fracture healing in an ovariectomized mice model.* BMC Musculoskeletal Disorders, 2021. **22**(1): p. 494.

83. Stegen, S., N. van Gastel, and G. Carmeliet, *Bringing new life to damaged bone: The importance of angiogenesis in bone repair and regeneration.* Bone, 2015. **70**: p. 19-27.

84. Lu, C., R. Marcucio, and T. Miclau, *Assessing Angiogenesis during Fracture Healing.* The Iowa Orthopaedic Journal, 2006. **26**: p. 17.

85. Ehnert, S., et al., *Effects of immune cells on mesenchymal stem cells during fracture healing.* World Journal of Stem Cells, 2021. **13**(11): p. 1667-1695.

86. Pacifici, R., *T cells, osteoblasts, and osteocytes: interacting lineages key for the bone anabolic and catabolic activities of parathyroid hormone.* Annals of the New York Academy of Sciences, 2016. **1364**(1): p. 11-24.

87. O'Gradaigh, D. and J.E. Compston, *T-cell involvement in osteoclast biology: implications for rheumatoid bone erosion.* Rheumatology, 2004. **43**(2): p. 122-130.

88. El Khassawna, T., et al., *T Lymphocytes Influence the Mineralization Process of Bone.* Frontiers in Immunology, 2017. **8**.

89. Singh, A., A.A. Mehdi, R.N. Srivastava, and N.S. Verma, *Immunoregulation of bone remodelling.* International Journal of Critical Illness and Injury Science, 2012. **2**(2): p. 75.

90. Li, M., et al., *Regulation of osteogenesis and osteoclastogenesis by zoledronic acid loaded on biodegradable magnesium-strontium alloy.* Scientific Reports, 2019. **9**(1): p. 933.

91. Chow, S.K.-H., et al., *Modulating macrophage polarization for the enhancement of fracture healing, a systematic review.* Journal of Orthopaedic Translation, 2022. **36**: p. 83-90.

92. Wernersson, S. and G. Pejler, *Mast cell secretory granules: armed for battle.* Nature Reviews Immunology, 2014. **14**(7): p. 478-494.

93. Yong, L.C.J., *The mast cell: origin, morphology, distribution, and function.* Experimental and Toxicologic Pathology, 1997. **49**(6): p. 409-424.

94. Vukman, K.V., et al., *Mast cell secretome: Soluble and vesicular components.* Seminars in Cell & Developmental Biology, 2017. **67**: p. 65-73.

95. Caughey, G.H., *Mast cell tryptases and chymases in inflammation and host defense.* Immunological Reviews, 2007. **217**(1): p. 141-154.

96. Moon, T.C., A.D. Befus, and M. Kulka, *Mast Cell Mediators: Their Differential Release and the Secretory Pathways Involved.* Frontiers in Immunology, 2014. **5**.

97. Ragipoglu, D., et al., *The Role of Mast Cells in Bone Metabolism and Bone Disorders.* Frontiers in Immunology, 2020. **11**: p. 163.

98. Kroner, J., et al., *Mast Cells Are Critical Regulators of Bone Fracture–Induced Inflammation and Osteoclast Formation and Activity.* Journal of Bone and Mineral Research, 2017. **32**(12): p. 2431-2444.

99. Lunderius-Andersson, C., M. Enoksson, and G. Nilsson, *Mast Cells Respond to Cell Injury through the Recognition of IL-33.* Frontiers in Immunology, 2012. **3**: p. 82.

100. Agier, J., J. Pastwińska, and E. Brzezińska-Błaszczyk, *An overview of mast cell pattern recognition receptors.* Inflammation Research, 2018. **67**(9): p. 737-746.

101. Xu, J., et al., *IL-23, but not IL-12, plays a critical role in inflammation-mediated bone disorders.* Theranostics, 2020. **10**(9): p. 3925-3938.

102. Chen, G., C. Deng, and Y.-P. Li, *TGF-β and BMP Signaling in Osteoblast Differentiation and Bone Formation.* International Journal of Biological Sciences, 2012. **8**(2): p. 272-288.

103. Mukai, K., M. Tsai, H. Saito, and S.J. Galli, *Mast cells as sources of cytokines, chemokines and growth factors.* Immunological reviews, 2018. **282**(1): p. 121-150.

104. Crivellato, E. and D. Ribatti, *Role of Mast Cells in Angiogenesis*, in *Biochemical Basis and Therapeutic Implications of Angiogenesis*, J.L. Mehta and N.S. Dhalla, Editors. 2013, Springer: New York, NY. p. 107-121.

105. Biosse-Duplan, M., et al., *Histamine Promotes Osteoclastogenesis through the Differential Expression of Histamine Receptors on Osteoclasts and Osteoblasts.* The American Journal of Pathology, 2009. **174**(4): p. 1426-1434.

106. Bonafede, M., D. Espindle, and A.G. Bower, *The direct and indirect costs of long bone fractures in a working age US population.* Journal of Medical Economics, 2013. **16**(1): p. 169-178.

107. Hak, D.J., et al., *Delayed union and nonunions: epidemiology, clinical issues, and financial aspects.* Injury, 2014. **45 Suppl 2**: p. S3-7.

108. Nicholson, J.A., N. Makaram, A. Simpson, and J.F. Keating, *Fracture nonunion in long bones: A literature review of risk factors and surgical management.* Injury, 2021. **52**: p. S3-S11.

109. Hoskins, W., et al., *The effect of patient, fracture and surgery on outcomes of high energy neck of femur fractures in patients aged 15–50.* HIP International, 2019. **29**(1): p. 77-82.

110. Brinker, M.R. and D.P. O'Connor, *The Biological Basis for Nonunions.* JBJS Reviews, 2016. **4**(6): p. e3.

111. Ali, A., H. Douglas, and D. Stanley, *Revision surgery for nonunion after early failure of fixation of fractures of the distal humerus.* The Journal of Bone and Joint Surgery. British Volume, 2005. **87**(8): p. 1107-1110.

112. Michel, P.A., et al., *Outcome after operative revision of clavicular nonunions.* Obere Extremität, 2020. **15**(1): p. 28-34.

113. Sahu, R.L., *Percutaneous autogenous bone marrow injection for delayed union or non-union of long bone fractures after internal fixation.* Revista Brasileira de Ortopedia, 2017. **53**(6): p. 668-673.

114. Conway, J.D., L. Shabtai, A. Bauernschub, and S.C. Specht, *BMP-7 versus BMP-2 for the treatment of long bone nonunion.* Orthopedics, 2014. **37**(12): p. e1049-1057.

115. Fuchs, T., et al., *Effect of Bone Morphogenetic Protein-2 in the Treatment of Long Bone Non-Unions.* Journal of Clinical Medicine, 2021. **10**(19): p. 4597.

116. Croes, M., B.C.H. van der Wal, and H.C. Vogely, *Impact of Bacterial Infections on Osteogenesis: Evidence From In Vivo Studies.* Journal of Orthopaedic Research, 2019. **37**(10): p. 2067-2076.

117. James, A.W., et al., *A Review of the Clinical Side Effects of Bone Morphogenetic Protein-2.* Tissue Engineering. Part B, Reviews, 2016. **22**(4): p. 284-297.

118. Yaw Tee, L.Y., S. Hunter, and J.F. Baker, *BMP use in the surgical treatment of pyogenic spondylodiscitis: Is it safe?* Journal of Clinical Neuroscience: Official Journal of the Neurosurgical Society of Australasia, 2022. **95**: p. 94-98.

119. Ahmed, E.M., *Hydrogel: Preparation, characterization, and applications: A review.* Journal of Advanced Research, 2015. **6**(2): p. 105-121.

120. Short, A.R., et al., *Hydrogels That Allow and Facilitate Bone Repair, Remodeling, and Regeneration.* Journal of materials chemistry. B, Materials for biology and medicine, 2015. **3**(40): p. 7818-7830.

121. Vigata, M., C. Meinert, D.W. Hutmacher, and N. Bock, *Hydrogels as Drug Delivery Systems: A Review of Current Characterization and Evaluation Techniques.* Pharmaceutics, 2020. **12**(12): p. 1188.

122. Sánchez-Cid, P., et al., *Biocompatible and Thermoresistant Hydrogels Based on Collagen and Chitosan.* Polymers, 2022. **14**(2): p. 272.

123. Gull, N., et al., *In vitro study of chitosan-based multi-responsive hydrogels as drug release vehicles: a preclinical study.* RSC Advances, 2019. **9**(53): p. 31078-31091.

124. Gull, N., et al., *Designing of biocompatible and biodegradable chitosan based crosslinked hydrogel for in vitro release of encapsulated povidone-iodine: A clinical translation.* International Journal of Biological Macromolecules, 2020. **164**: p. 4370-4380.

125. Jacob, S., et al., *Emerging Role of Hydrogels in Drug Delivery Systems, Tissue Engineering and Wound Management.* Pharmaceutics, 2021. **13**(3): p. 357.

126. Klouda, L., *Thermoresponsive hydrogels in biomedical applications: A seven-year update.* European Journal of Pharmaceutics and Biopharmaceutics: Official Journal of Arbeitsgemeinschaft Fur Pharmazeutische Verfahrenstechnik e.V, 2015. **97**(Pt B): p. 338-349.

127. McKenzie, M., et al., *Hydrogel-Based Drug Delivery Systems for Poorly Water-Soluble Drugs.* Molecules, 2015. **20**(11): p. 20397-20408.

128. Tabata, Y., *Biomaterial technology for tissue engineering applications.* Journal of the Royal Society, Interface, 2009. **6 Suppl 3**(Suppl 3): p. S311-324.

129. parhi, R., *Cross-Linked Hydrogel for Pharmaceutical Applications: A Review.* Advanced Pharmaceutical Bulletin, 2017. **7**(4): p. 515-530.

130. Bashir, S., et al., *Fundamental Concepts of Hydrogels: Synthesis, Properties, and Their Applications.* Polymers, 2020. **12**(11): p. 2702.

131. Tang, S., et al., *Chapter 3 - Physical hydrogels based on natural polymers*, in *Hydrogels Based on Natural Polymers*, Y. Chen, Editor. 2020, Elsevier. p. 51-89.

132. Lee, K.Y. and D.J. Mooney, *Alginate: properties and biomedical applications.* Progress in polymer science, 2012. **37**(1): p. 106-126.

133. López-Marcial, G.R., et al., *Agarose-Based Hydrogels as Suitable Bioprinting Materials for Tissue Engineering.* ACS Biomaterials Science & Engineering, 2018. **4**(10): p. 3610-3616.

134. Ward, M.A. and T.K. Georgiou, *Thermoresponsive Polymers for Biomedical Applications.* Polymers, 2011. **3**(3): p. 1215-1242.

135. Pepelanova, I., *Tunable Hydrogels: Introduction to the World of Smart Materials for Biomedical Applications.* Advances in Biochemical Engineering/Biotechnology, 2021. **178**: p. 1-35.

136. Liu, X., et al., *Therapeutic application of hydrogels for bone-related diseases.* Frontiers in Bioengineering and Biotechnology, 2022. **10**: p. 998988.

137. Ji, X., et al., *Mesenchymal stem cell-loaded thermosensitive hydroxypropyl chitin hydrogel combined with a three-dimensional-printed poly(ε-caprolactone) /nano-hydroxyapatite*

scaffold to repair bone defects via osteogenesis, angiogenesis and immunomodulation. Theranostics, 2020. **10**(2): p. 725-740.

138. Bai, L., et al., *Hydrogel Drug Delivery Systems for Bone Regeneration.* Pharmaceutics, 2023. **15**(5): p. 1334.

139. Wang, B., et al., *Mussel-Inspired Bisphosphonated Injectable Nanocomposite Hydrogels with Adhesive, Self-Healing, and Osteogenic Properties for Bone Regeneration.* ACS applied materials & interfaces, 2021. **13**(28): p. 32673-32689.

140. Chen, Y., et al., *Magnesium Oxide Nanoparticle Coordinated Phosphate-Functionalized Chitosan Injectable Hydrogel for Osteogenesis and Angiogenesis in Bone Regeneration.* ACS applied materials & interfaces, 2022. **14**(6): p. 7592-7608.

141. Willie, B.M., et al., *Designing biomimetic scaffolds for bone regeneration: why aim for a copy of mature tissue properties if nature uses a different approach?* Soft Matter, 2010. **6**(20): p. 4976-4987.

142. Puppi, D., F. Chiellini, A.M. Piras, and E. Chiellini, *Polymeric materials for bone and cartilage repair.* Progress in Polymer Science, 2010. **35**(4): p. 403-440.

143. Liu, X. and P.X. Ma, *Polymeric scaffolds for bone tissue engineering.* Annals of Biomedical Engineering, 2004. **32**(3): p. 477-486.

144. BaoLin, G. and P.X. Ma, *Synthetic biodegradable functional polymers for tissue engineering: a brief review.* Science China. Chemistry, 2014. **57**(4): p. 490-500.

145. Zhang, Y., et al., *In situ bone regeneration enabled by a biodegradable hybrid double-network hydrogel.* Biomaterials Science, 2019. **7**(8): p. 3266-3276.

146. Olov, N., S. Bagheri-Khoulenjani, and H. Mirzadeh, *Injectable hydrogels for bone and cartilage tissue engineering: a review.* Progress in Biomaterials, 2022. **11**: p. 113-135.

147. Bodratti, A.M. and P. Alexandridis, *Formulation of Poloxamers for Drug Delivery.* Journal of Functional Biomaterials, 2018. **9**(1): p. 11.

148. Russo, E. and C. Villa, *Poloxamer Hydrogels for Biomedical Applications.* Pharmaceutics, 2019. **11**(12): p. 671.

149. Wang, P., et al., *Effects of Pluronic F127-PEG multi-gel-core on the release profile and pharmacodynamics of Exenatide loaded in PLGA microspheres.* Colloids Surf B Biointerfaces, 2016. **147**: p. 360-367.

150. Ferris, C.J., K.J. Gilmore, G.G. Wallace, and M.i.h. Panhuis, *Modified gellan gum hydrogels for tissue engineering applications.* Soft Matter, 2013. **9**(14): p. 3705-3711.

151. Sworn, G., G.R. Sanderson, and W. Gibson, *Gellan gum fluid gels.* Food Hydrocolloids, 1995. **9**(4): p. 265-271.

152. Das, M. and T.K. Giri, *Hydrogels based on gellan gum in cell delivery and drug delivery.* Journal of Drug Delivery Science and Technology, 2020. **56**: p. 101586.

153. Coutinho, D.F., et al., *Modified Gellan Gum hydrogels with tunable physical and mechanical properties.* Biomaterials, 2010. **31**(29): p. 7494-7502.

154. Silva, E., et al., *Proteins encoded by Sphingomonas elodea ATCC 31461 rmlA and ugpG genes, involved in gellan gum biosynthesis, exhibit both dTDP- and UDP-glucose pyrophosphorylase activities.* Applied and Environmental Microbiology, 2005. **71**(8): p. 4703-4712.

155. Nayak, A.K., et al., *Chapter 13 - Gellan gum-based nanomaterials in drug delivery applications*, in *Biopolymer-Based Nanomaterials in Drug Delivery and Biomedical Applications*, H. Bera, C.M. Hossain, and S. Saha, Editors. 2021, Academic Press. p. 313-336.

156. Kirchmajer, D.M., et al., *Enhanced gelation properties of purified gellan gum.* Carbohydrate Research, 2014. **388**: p. 125-129.

157. Sandford, P.A., I.W. Cottrell, and D.J. Pettitt, *Microbial polysaccharides: new products and their commercial applications.* Pure and Applied Chemistry, 1984. **56**(7): p. 879-892.

158. Muthukumar, T., J.E. Song, and G. Khang, *Biological Role of Gellan Gum in Improving Scaffold Drug Delivery, Cell Adhesion Properties for Tissue Engineering Applications.* Molecules, 2019. **24**(24): p. 4514.

159. Cui, L., et al., *Injectable and Degradable POSS–Polyphosphate–Polysaccharide Hybrid Hydrogel Scaffold for Cartilage Regeneration.* ACS Applied Materials & Interfaces, 2023. **15**(17): p. 20625-20637.

160. Hu, X., L. Zhang, L. Yan, and L. Tang, *Recent Advances in Polysaccharide-Based Physical Hydrogels and Their Potential Applications for Biomedical and Wastewater Treatment.* Macromolecular Bioscience, 2022. **22**(9): p. e2200153.

161. Hao, Y., et al., *A fully degradable and photocrosslinked polysaccharide-polyphosphate hydrogel for tissue engineering.* Carbohydrate Polymers, 2019. **225**: p. 115257.

162. Wu, A.T., et al., *Enhancing osteogenic differentiation of MC3T3-E1 cells by immobilizing inorganic polyphosphate onto hyaluronic acid hydrogel.* Biomacromolecules, 2015. **16**(1): p. 166-73.

163. Wang, X., H.C. Schroder, and W.E.G. Muller, *Amorphous polyphosphate, a smart bioinspired nano-/bio-material for bone and cartilage regeneration: towards a new paradigm in tissue engineering.* J Mater Chem B, 2018. **6**(16): p. 2385-2412.

164. Muller, W.E.G., et al., *Amorphous, Smart, and Bioinspired Polyphosphate Nano/Microparticles: A Biomaterial for Regeneration and Repair of Osteo-Articular Impairments In-Situ.* Int J Mol Sci, 2018. **19**(2).

165. Claes, L., S. Recknagel, and A. Ignatius, *Fracture healing under healthy and inflammatory conditions.* Nature Reviews. Rheumatology, 2012. **8**(3): p. 133-143.

166. Axelrad, T.W. and T.A. Einhorn, *Bone morphogenetic proteins in orthopaedic surgery.* Cytokine & Growth Factor Reviews, 2009. **20**(5-6): p. 481-488.

167. Müller, W.E.G., H.C. Schröder, and X. Wang, *Inorganic Polyphosphates As Storage for and Generator of Metabolic Energy in the Extracellular Matrix.* Chemical Reviews, 2019. **119**(24): p. 12337-12374.

168. Müller, F., et al., *Platelet polyphosphates are proinflammatory and procoagulant mediators in vivo.* Cell, 2009. **139**(6): p. 1143-1156.

169. Bae, J.S., W. Lee, and A.R. Rezaie, *Polyphosphate elicits pro-inflammatory responses that are counteracted by activated protein C in both cellular and animal models.* Journal of Thrombosis and Haemostasis, 2012. **10**(6): p. 1145-1151.

170. Morrissey, J.H., S.H. Choi, and S.A. Smith, *Polyphosphate: an ancient molecule that links platelets, coagulation, and inflammation.* Blood, 2012. **119**(25): p. 5972-5979.

171. Azouz, N.P., I. Hammel, and R. Sagi-Eisenberg, *Characterization of Mast Cell Secretory Granules and Their Cell Biology.* DNA and Cell Biology, 2014. **33**(10): p. 647-651.

172. Hurst, S.M., et al., *Il-6 and its soluble receptor orchestrate a temporal switch in the pattern of leukocyte recruitment seen during acute inflammation.* Immunity, 2001. **14**(6): p. 705-714.

173. Prabaharan, M., J.J. Grailer, D.A. Steeber, and S. Gong, *Stimuli-Responsive Chitosan-graft-Poly(N-vinylcaprolactam) as a Promising Material for Controlled Hydrophobic Drug Delivery.* Macromolecular Bioscience, 2008. **8**(9): p. 843-851.

174. Indulekha, S., P. Arunkumar, D. Bahadur, and R. Srivastava, *Thermoresponsive polymeric gel as an on-demand transdermal drug delivery system for pain management.* Materials Science and Engineering: C, 2016. **62**: p. 113-122.

175. Shiu, H.T., P.C. Leung, and C.H. Ko, *The roles of cellular and molecular components of a hematoma at early stage of bone healing.* Journal of Tissue Engineering and Regenerative Medicine, 2018. **12**(4): p. e1911-e1925.

176. Yun, S.H., et al., *Platelet Activation: The Mechanisms and Potential Biomarkers.* Biomed Res Int, 2016. **2016**: p. 9060143.

177. Smith, S.A., et al., *Polyphosphate modulates blood coagulation and fibrinolysis.* Proceedings of the National Academy of Sciences, 2006. **103**(4): p. 903-908.

178. Dinarvand, P., et al., *Polyphosphate amplifies proinflammatory responses of nuclear proteins through interaction with receptor for advanced glycation end products and P2Y1 purinergic receptor.* Blood, 2014. **123**(6): p. 935-45.

179. Krenzlin, V., et al., *Immunomodulation of neutrophil granulocyte functions by bacterial polyphosphates.* Eur J Immunol, 2023. **53**(5): p. e2250339.

180. Halova, I., L. Draberova, and P. Draber, *Mast cell chemotaxis - chemoattractants and signaling pathways.* Front Immunol, 2012. **3**: p. 119.

181. Shimizu, T., et al., *TRPM4 regulates migration of mast cells in mice.* Cell Calcium, 2009. **45**(3): p. 226-32.

182. da Silva, L.P., et al., *Engineering cell-adhesive gellan gum spongy-like hydrogels for regenerative medicine purposes.* Acta Biomaterialia, 2014. **10**(11): p. 4787-4797.

183. El-Jawhari, J.J., E. Jones, and P.V. Giannoudis, *The roles of immune cells in bone healing; what we know, do not know and future perspectives.* Injury, 2016. **47**(11): p. 2399-2406.

184. Abdeltawab, H., D. Svirskis, and M. Sharma, *Formulation strategies to modulate drug release from poloxamer based in situ gelling systems.* Expert Opinion on Drug Delivery, 2020. **17**(4): p. 495-509.

185. Shinsho, A., et al., *The thickening properties of native gellan gum are due to freeze drying–induced aggregation.* Food Hydrocolloids, 2020. **109**: p. 105997.

186. Ozpinar, E.W., A.L. Frey, G. Cruse, and D.O. Freytes, *Mast Cell–Biomaterial Interactions and Tissue Repair.* Tissue Engineering Part B: Reviews, 2021. **27**(6): p. 590-603.

187. De Filippo, K., et al., *Mast cell and macrophage chemokines CXCL1/CXCL2 control the early stage of neutrophil recruitment during tissue inflammation.* Blood, 2013. **121**(24): p. 4930-4937.

188. West, P.W. and S. Bulfone-Paus, *Mast cell tissue heterogeneity and specificity of immune cell recruitment.* Frontiers in Immunology, 2022. **13**: p. 932090.

189. Zechner, C. and U. Gruntmanis, *Systemic Mastocytosis With Decreased Bone Density and Fractures.* Mayo Clinic Proceedings, 2015. **90**(6): p. 843-844.

190. Ragipoglu, D., et al., *Mast Cells Drive Systemic Inflammation and Compromised Bone Repair After Trauma.* Frontiers in Immunology, 2022. **13**.

191. Behrends, D.A., et al., *Defective Bone Repair in C57Bl6 Mice With Acute Systemic Inflammation.* Clinical Orthopaedics and Related Research, 2017. **475**(3): p. 906-916.

192. Ramirez-GarciaLuna, J.L., et al., *Enhanced Bone Remodeling After Fracture Priming.* Calcified Tissue International, 2022. **110**(3): p. 349-366.

193. Ramirez-Garcia-Luna, J.L., et al., *Defective bone repair in diclofenac treated C57Bl6 mice with and without lipopolysaccharide induced systemic inflammation.* Journal of Cellular Physiology, 2019. **234**(3): p. 3078-3087.

194. Qu, H., H. Fu, Z. Han, and Y. Sun, *Biomaterials for bone tissue engineering scaffolds: a review.* RSC Advances. **9**(45): p. 26252-26262.

195. Girón, J., et al., *Biomaterials for bone regeneration: an orthopedic and dentistry overview.* Brazilian Journal of Medical and Biological Research, 2021. **54**(9): p. e11055.

196. Herr, N., C. Bode, and D. Duerschmied, *The Effects of Serotonin in Immune Cells.* Frontiers in Cardiovascular Medicine, 2017. **4**.

197. Falcone, F.H., D. Wan, N. Barwary, and R. Sagi-Eisenberg, *RBL cells as models for in vitro studies of mast cells and basophils.* Immunological Reviews, 2018. **282**(1): p. 47-57.

198. Cynthia, J.M., et al., *The c-kit Receptor Ligand Functions as a Mast Cell Chemoattractant.* Blood, 1992. **79**(4): p. 958-963.

199. Da Silva, C.A., L. Reber, and N. Frossard, *Stem cell factor expression, mast cells and inflammation in asthma.* Fundamental & Clinical Pharmacology, 2006. **20**(1): p. 21-39.

200. Jin, J., V.R. Dasari, F.D. Sistare, and S.P. Kunapuli, *Distribution of P2Y receptor subtypes on haematopoietic cells.* British Journal of Pharmacology, 1998. **123**(5): p. 789-794.

201. Baryshnikov, S.G., O.A. Rogachevskaja, and S.S. Kolesnikov, *Calcium signaling mediated by P2Y receptors in mouse taste cells.* Journal of Neurophysiology, 2003. **90**(5): p. 3283-3294.

202. Glaser, T., R.R. Resende, and H. Ulrich, *Implications of purinergic receptor-mediated intracellular calcium transients in neural differentiation.* Cell Communication and Signaling, 2013. **11**(1): p. 12.

203. Elieh Ali Komi, D., S. Wöhrl, and L. Bielory, *Mast Cell Biology at Molecular Level: a Comprehensive Review.* Clinical Reviews in Allergy & Immunology, 2020. **58**(3): p. 342-365.

204. Wang, L., S.E.W. Jacobsen, A. Bengtsson, and D. Erlinge, *P2 receptor mRNA expression profiles in human lymphocytes, monocytes and CD34+ stem and progenitor cells.* BMC immunology, 2004. **5**: p. 16.

205. Layhadi, J.A. and S.J. Fountain, *ATP-Evoked Intracellular Ca2+ Responses in M-CSF Differentiated Human Monocyte-Derived Macrophage are Mediated by P2X4 and P2Y11 Receptor Activation.* International Journal of Molecular Sciences, 2019. **20**(20): p. 5113.

206. Klaver, D. and M. Thurnher, *Control of Macrophage Inflammation by P2Y Purinergic Receptors.* Cells, 2021. **10**(5): p. 1098.

207. Bakhti, M., et al., *Loss of electrostatic cell-surface repulsion mediates myelin membrane adhesion and compaction in the central nervous system.* Proceedings of the National Academy of Sciences of the United States of America, 2013. **110**(8): p. 3143-3148.

208. Ma, Y., K. Poole, J. Goyette, and K. Gaus, *Introducing Membrane Charge and Membrane Potential to T Cell Signaling.* Frontiers in Immunology, 2017. **8**: p. 1513.

209. Zhan, J., et al., *Preparation and Antibacterial Activity of Thermo-Responsive Nanohydrogels from Qiai Essential Oil and Pluronic F108.* Molecules (Basel, Switzerland), 2021. **26**(19): p. 5771.

210. Rahman, M.S., et al., *Morphological Characterization of Hydrogels*, in *Cellulose-Based Superabsorbent Hydrogels*, M.I.H. Mondal, Editor. 2019, Springer International Publishing: Cham. p. 819-863.

211. Santana, B.P., et al., *Comparing different methods to fix and to dehydrate cells on alginate hydrogel scaffolds using scanning electron microscopy.* Microscopy Research and Technique, 2015. **78**(7): p. 553-561.

212. Norrby, K., *Mast cells and angiogenesis.* APMIS: acta pathologica, microbiologica, et immunologica Scandinavica, 2002. **110**(5): p. 355-371.

213. Antebi, B., et al., *Controlling Arteriogenesis and Mast Cells Are Central to Bioengineering Solutions for Critical Bone Defect Repair Using Allografts.* Bioengineering, 2016. **3**(1): p. 6.

214. Maruyama, M., et al., *Modulation of the Inflammatory Response and Bone Healing.* Frontiers in Endocrinology, 2020. **11**: p. 386.

215. Lin, X., S. Patil, Y.G. Gao, and A. Qian, *The Bone Extracellular Matrix in Bone Formation and Regeneration.* Front Pharmacol, 2020. **11**: p. 757.

216. Grzeskowiak, R.M., et al., *Bone and Cartilage Interfaces With Orthopedic Implants: A Literature Review.* Front Surg, 2020. **7**: p. 601244.

217. Fadini, G.P., M. Albiero, B.M. Bonora, and A. Avogaro, *Angiogenic Abnormalities in Diabetes Mellitus: Mechanistic and Clinical Aspects.* J Clin Endocrinol Metab, 2019. **104**(11): p. 5431-5444.

218. Peng, G.L., *Platelet-Rich Plasma for Skin Rejuvenation: Facts, Fiction, and Pearls for Practice.* Facial Plast Surg Clin North Am, 2019. **27**(3): p. 405-411.

219. Conde Montero, E., M.E. Fernandez Santos, and R. Suarez Fernandez, *Platelet-rich plasma: applications in dermatology.* Actas Dermosifiliogr, 2015. **106**(2): p. 104-11.

220. Wu, P.I., R. Diaz, and J. Borg-Stein, *Platelet-Rich Plasma.* Phys Med Rehabil Clin N Am, 2016. **27**(4): p. 825-853.

221. Nishio, H., et al., *Platelet-rich plasma promotes recruitment of macrophages in the process of tendon healing.* Regen Ther, 2020. **14**: p. 262-270.

222. Yu, T., et al., *Autologous platelet-rich plasma induces bone formation of tissue-engineered bone with bone marrow mesenchymal stem cells on beta-tricalcium phosphate ceramics.* Journal of Orthopaedic Surgery and Research, 2017. **12**(1): p. 178.

223. Mishra, A., et al., *Buffered platelet-rich plasma enhances mesenchymal stem cell proliferation and chondrogenic differentiation.* Tissue Engineering. Part C, Methods, 2009. **15**(3): p. 431-435.

224. Kabiri, A., et al., *Platelet-rich plasma application in chondrogenesis.* Advanced Biomedical Research, 2014. **3**: p. 138.

225. Pavlovic, V., M. Ciric, V. Jovanovic, and P. Stojanovic, *Platelet Rich Plasma: a short overview of certain bioactive components.* Open Medicine, 2016. **11**(1): p. 242-247.

A thesis submitted to McGill University in partial fulfillment of the requirements of the degree of Master of Science in Surgical and Interventional Sciences